The state-of-the-art in ultrasound-guided spine interventions

Houssem-Eddine Gueziri[a,c], Carlo Santaguida[b], D. Louis Collins[a,c]

[a] *McConnell Brain Imaging Center, Montreal Neurological Institute and Hospital, Montreal (QC), Canada.*
[b] *Department of Neurology and Neurosurgery, McGill University Health Center, Montreal (QC), Canada.*
[c] *McGill University, Montreal (QC), Canada.*

Abstract

During the last two decades, intra-operative ultrasound (iUS) imaging has been employed for various surgical procedures of the spine, including spinal fusion and needle injections. Accurate and efficient registration of pre-operative computed tomography or magnetic resonance images with iUS images are key elements in the success of iUS-based spine navigation. While widely investigated in research, iUS-based spine navigation has not yet been established in the clinic. This is due to several factors including the lack of a standard methodology for the assessment of accuracy, robustness, reliability, and usability of the registration method. To address these issues, we present a systematic review of the state-of-the-art techniques for iUS-guided registration in spinal image-guided surgery (IGS). The review follows a new taxonomy based on the four steps involved in the surgical workflow that include pre-processing, registration initialization, estimation of the required patient to image transformation, and a visualization process. We provide a detailed analysis of the measurements in terms of accuracy, robustness, reliability, and usability that need to be met during the evaluation of a spinal IGS framework. Although this review is focused on spinal navigation, we expect similar evaluation criteria to be relevant for other IGS applications.

Keywords: Spine intervention, Intraoperative ultrasound, Image registration, Image-guided surgery

1. Introduction

Many pathologic factors such as traumatic, metabolic, toxic, genetic, vascular, and infectious factors are identified as causes of degenerative changes of the spine responsible for spinal instability (Gallucci et al., 2007). When medication and physical therapy fail, patients with spinal instability may consider undergoing surgery, in which a spinal fusion procedure is required to correct a spine deformity or to sustain the spine structure post-operatively. The surgery consists in rigidly fusing multiple vertebrae using rods and bone grafts to help stabilize the spinal column. The rods are fixed to each vertebra using screws implanted within the vertebral pedicles. A pre-operative computed tomography (CT), intraoperative CT, or intraoperative 3D fluoroscopy is often used to plan the entry point and trajectory of the pedicle screws. During surgery, the posterior part of the vertebra is exposed and the surgeon is required to mentally align the drilling trajectory to match the surgical planning, based on knowledge of patient's anatomy (Merloz et al., 1997). Often 2D fluoroscopy is used to refine pedicle screw trajectories to prevent erroneous placement of a pedicle screw. Despite 2D fluoroscopy, there is still a small but significant risk of screw misplacement (Kast et al., 2006; Di Silvestre et al., 2007; Şarlak et al., 2009; Hicks et al., 2010; Gelalis et al., 2012).

During the last two decades, the number of annual spinal fusion procedures has known a significant increase in the United States, where over 413,000 interventions were reported in 2008 (Rajaee and Delamarter, 2012), with a 56.4 % increase between 2003 and 2012 (Bernstein et al., 2017). This trend is supported by the development of new technologies for navigated instrumentation, reducing risks of neurological and vascular complications associated with screw malpositioning, involving pedicle fractures, weak/loose fixation, pleural effusion, dural tears and wound infections (Smith et al., 2014; Gebhard et al., 2004; Austin et al., 2002). Moreover, advanced techniques involving minimally invasive spine surgery for spinal fusion have been considered using computer-assisted navigation systems. Such systems are categorized into three groups: 1) passive

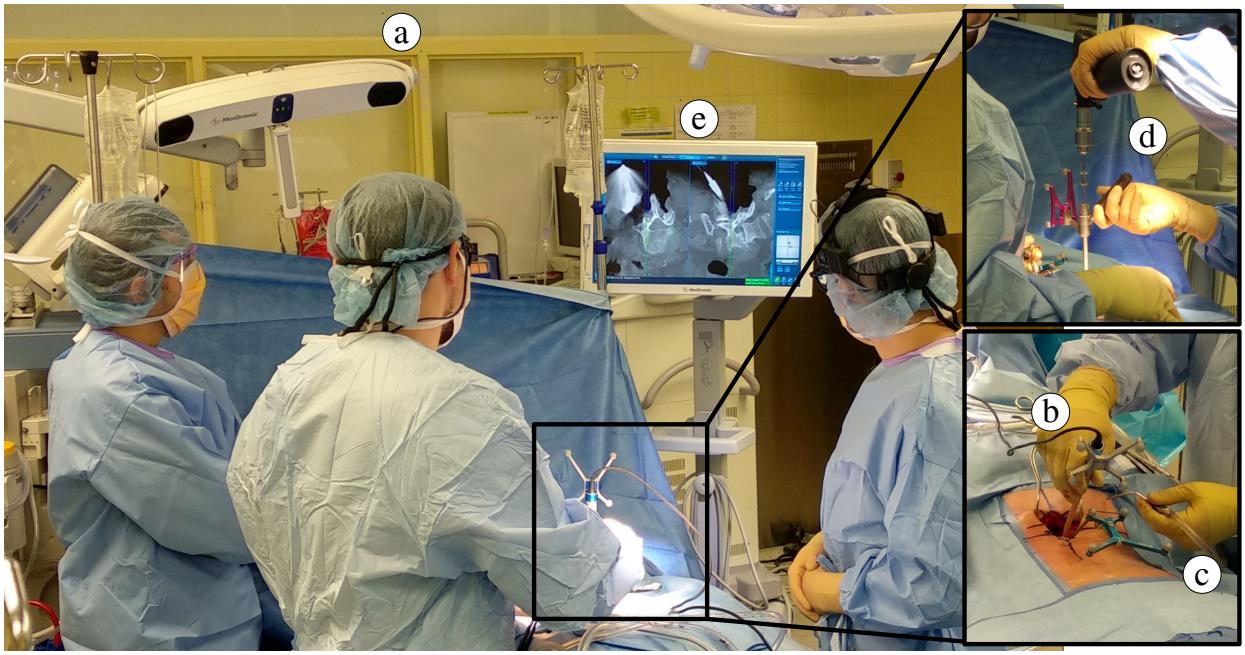

Figure 1: Image guided surgery system: (a) tracking camera, (b) tracked pointer, (c) dynamic reference object (DRO), (d) tracked instrument (drill) and (e) computer station.

navigation provides the surgeon with real-time spatial position of surgical instruments with respect to the patient anatomy, without interfering with the surgeon's action; 2) semi-active navigation limits the surgeon to only perform pre-operatively planned actions; 3) active navigation performs pre-operatively planned actions without surgeon interaction. For spine surgery, the current clinical practice is based on passive navigation using image-guided surgery (IGS) that allows visualization of the projected drilling trajectory and the surgical plan to assist the surgeon to find the optimal entry point and angular orientation of the pedicle screw.

1.1. Image-guided spine surgery

A typical IGS system consists of three major components (see Fig. 1): 1) a tracking device, 2) tracked tools, and 3) a computer station. Most tracking devices rely on an optical tracking camera to localize infrared light-emitting diodes or infrared light-reflecting spheres, rigidly fixed to surgical instruments (i.e., tracked tools), to determine their spatial positions in the operative field. Note that alternative tracking systems use electromagnetic (Sagi et al., 2003) or ultrasonic (O'Donnell et al., 1994; Laurijssen et al., 2017) technologies, but are less frequent in spine surgery. In addition to the instruments needed for surgery, the navigation system tracks a pointer (or stylus) and dynamic reference object (DRO). The pointer is calibrated prior to the surgery so that the 3D coordinate of the pointer tip is known by the navigation system, and is commonly used to identify 3D points on the patient's anatomy. The DRO is a rigid body, tracked by the camera, that is attached to the spinous process of a neighboring vertebra or iliac bone and serves as a coordinate reference frame. Tracking information is sent to a computer station, in which pre-operative images are aligned with the tracked instruments and visualized in real-time.

To allow navigation, a key step in IGS is finding the corresponding spatial transformation between preoperative images and the current patient anatomy. A straightforward method to estimate this transformation is to use manual landmark-based registration. This is done by using the pointer to locate physical landmarks on the patient anatomy, usually, the tips of transverse processes and spinous processes (Girardi et al., 1999), while the same landmarks are identified on the pre-operative images. A rigid transform is calculated by finding the pair-wise point correspondence. However, the rounded extremities of transverse and spinous

processes do not provide good landmark candidates that can be uniquely identified within the vertebra anatomy, thereby affecting the registration quality. Another approach is to use surface-based registration. Instead of locating specific landmarks on the vertebra, the surgeon collects a large number of points that lie on the surface of the vertebra. These points are registered with pre-computed surface points extracted from the pre-operative CT image. The time required to achieve manual landmark-based registration is estimated to be 10 to 15 min per vertebra (Yan et al., 2011) and the procedure may require significant surgical exposure of the vertebra. To obviate the need for this exposure, single element transducer ultrasound probes have been employed to collect surface points non-invasively (Carl et al., 1997; Mozes et al., 2010; Amstutz et al., 2003). While the approach is non-invasive, allowing vertebra registration in minimally invasive surgeries, the method inherits manual-registration limitations, i.e., the difficulty of locating candidate points and the long manual procedure time. In addition, because the acoustic device relies on acoustic impedance properties, a prior calibration is required to characterize the bone surface acoustic response, but this response depends on the patient bone properties and the incidence angle of the ultrasound beam, which may result in errors of surface location estimation.

In the early 2000s, intra-operative CT was employed to overcome the limitations of manual landmark identification on patient anatomy. Prior to the imaging, titanium screws (approximately, 2 mm diameter, 5 mm length) can be implanted into the vertebra to serve as fiducials for landmark-based registration. The screws appear on the CT images and their corresponding locations can be accurately collected using a tracked pointer (Haberland et al., 2000), however, these screws represent an additional invasive surgical manipulation just for registration. Current commercial navigation systems for spine surgery allow the acquisition of 2D fluoroscopy or 3D CT intra-operative images, e.g., the O-arm (Medtronic inc., Minneapolis, MN, USA), Airo Mobile (Brainlab, Feldkirchen, Germany), SpineMask (Stryker, Kalamazoo, MI, USA) or Ziehm Vision FD Vario 3D (Ziehm Imaging, Orlando, FL, USA). We refer interested readers to the recent survey of commercial robotic-assisted spine surgery systems (Overley et al., 2017). To achieve non-invasive patient alignment, the DRO is attached to the patient before CT imaging, which allows the DRO's reflective spheres to appear clearly on the CT images, facilitating their identification. The location of the spheres in the image coordinate frame is computed and used for registration with their corresponding tracked positions given by the tracking camera. The advantage of intraoperative CT is two-fold: First, the registration procedure is fully automated. Second, intra-operative CT provides updates of the patient anatomy during surgery (Rahmathulla et al., 2014; Gebhard et al., 2004; Costa et al., 2015), which accounts for patient movements and change in the spine curvature. Intraoperative CT can yield a sub-millimeter target registration error (TRE) of 0.80 mm $\pm$ 0.28 mm in spinal surgery (Carl et al., 2019a). However, the procedure introduces risks of potentially harmful radiation exposure for both the patient and the operating room (OR) personnel (Tabaraee et al., 2013; Rampersaud et al., 2000). In addition, the time required to achieve intra-operative CT imaging is 15-20 minutes, including the time needed for draping the patient, adjusting the surgical table, positioning the scanner, asking the staff to leave the OR for radiation safety, acquiring the images and removing the scanner. Despite causing a significant interruption of surgical workflow, the use of intra-operative CT imaging is becoming more accepted as a clinical routine for spine navigation in fusion surgery (Waschke et al., 2013).

Non-ionizing imaging modalities have been investigated as alternative solutions for spine navigation. Stereovision has been employed to reconstruct the exposed posterior surface of vertebrae and perform a surface-based registration with pre-operative CT and MR (Ji et al., 2015; Jakubovic et al., 2018; Guha et al., 2019b). While the collection of intra-operative anatomical surface points using stereovision is non-invasive, the technique requires significant exposition of the posterior part of the vertebra, precluding its application to minimally invasive surgery.

The use of intra-operative magnetic resonance (MR) imaging has been reported in a few cases in cervical spine surgery (Woodard et al., 2001), cyst fenestration (Takahashi et al., 2008, 2009) and spinal laser thermotherapy (Tatsui et al., 2017). Compared to fluoroscopy and CT imaging, MR imaging provides better visualization of soft tissues, nerves, and the spinal cord. However, utilization of intra-operative MR to perform spinal procedures remains very limited due to the high costs and the restrictive MR-compatibility constraints of OR equipment and surgical instruments.

Intra-operative ultrasound (iUS) has been widely used for image guidance in neurosurgery (Comeau

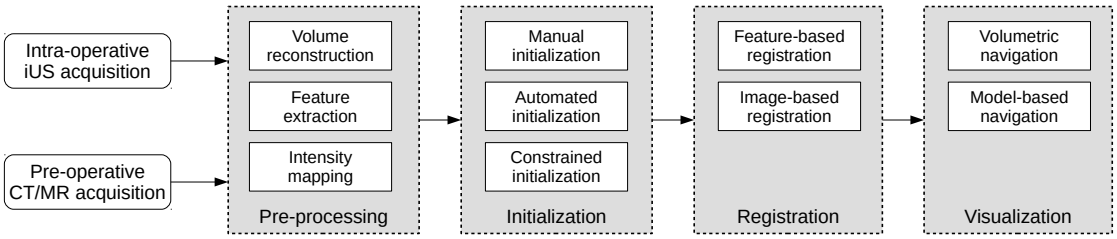

Figure 2: Workflow for CT-to-ultrasound registration.

et al., 2000; Unsgaard et al., 2006; Riva et al., 2017). The real-time acquisition provided by iUS imaging allows for the update of the local anatomy undergoing surgery to account for brain shift in tumor resection (Iversen et al., 2018; De Nigris et al., 2012; Nimsky et al., 2001), cerebral sparganosis removal (Nkwerem et al., 2017) or ventricular catheter insertion (Heussinger et al., 2013). In spine surgery, clinical feasibility of iUS imaging for the assessment of residual tumor after complete resection was investigated (Saß et al., 2019). Yet, the iUS images were only used for live visualization and the navigation (i.e., image-to-patient registration) was established using intraoperative CT. The development of standalone ultrasound-guided navigation systems has been hindered by the low quality of iUS images. The high density of the bone tissue induces strong absorption of the ultrasound signal. As a result, ultrasound images of bony structures appear as a hyperechoic region located at the bone-tissue interface followed by shadow artifacts caused by the signal drop off. For the complex anatomy of the vertebra, overlapping structures such as the inferior-superior articular processes are subject to occlusion. Moreover, the intensity of the signal response depends on the angle of incidence of the ultrasound beam when penetrating the bone. Hence, the image intensity may vary significantly along with the bone-tissue interface. Nevertheless, the practicality of iUS imaging for interventional applications encouraged the development of recent approaches for iUS-based spine navigation. The driving idea was not to interpret the images directly for diagnosis or guidance, but rather, to employ iUS imaging to collect anatomical features that are used to register the patient to pre-operative CT or MR diagnostic images. The goal of this paper is to review the iUS-based registration techniques that have been proposed for standard and minimally invasive spine interventions. Although this paper focuses on pedicle screw fixation, similar registration principles involved in iUS-based navigation apply for other procedures such as spinal needle injection, laminectomy or spinal decompression surgery, for example.

1.2. Ultrasound-based spine navigation

Figure 2 illustrates a typical iUS-based registration workflow. The registration framework consists of 4 blocks: the image pre-processing block, the initialization block, the registration block, and the visualization block. The pre-processing block covers all data preparation steps that are performed prior to registration. The second block concerns the initialization of the registration transform. This transform is often used as a rough starting point from which the final registration is refined in the third block. The fourth and final visualization or navigation block provides the surgeon with the display of surgical instruments overlaid on the pre-operative images. We will use this workflow to organize the review below. Measurements used for the validation of IGS navigation systems are discussed in Section 7. We consider evaluation criteria according to accuracy, robustness, reliability, and usability as suggested by Cleary et al. (2000).

2. Search methodology

Figure 3 shows a diagram of the search strategy used in this review. Following the Preferred Reporting Items for Systematic Reviews and Meta-Analyses (PRISMA) 2009 guidelines (Moher et al., 2009), we queried the PubMed database to which we manually added 37 selected references that were found relevant to the review. The following search request was used:

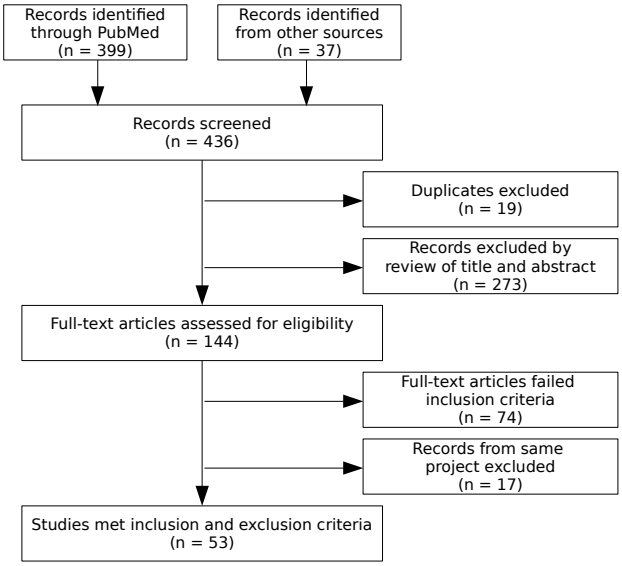

Figure 3: Selection process for studies included in the review.

```
((Spine OR Spinal OR Vertebra*) AND (Ultrasound OR Echograph*) AND (Registration OR Align*)
AND (navigat* OR guid*))
```

After duplicate removal, titles and abstracts of the resulting records were screened to eliminate non-English and irrelevant entries. The full-text of the remaining entries were assessed for eligibility focusing on works that address the registration problem of CT or MR to iUS images. The selection process involved the following inclusion/exclusion criteria: The work should involve the use of ultrasound as intra-operative imaging modality to perform spine navigation. The work should focus on spine applications: open-back surgery or minimally invasive spine surgery. This includes pedicle screw fixation and needle guidance for percutaneous spinal injections. Case studies are not included in this review. Finally, if work from a specific research group or project had been published more than once and without significant modifications, only the most recent publication was reviewed. In total, 53 articles satisfied these criteria and were selected for review following the four blocks or the workflow in Fig. 2.

A comprehensive description of the reported methods is shown in Table 1. The following criteria were taken into account: First, the type of registration indicates whether the registration processes multiple vertebrae as a single rigid-body/deformable or allows group-wise vertebra registration to compensate for spine curvature. In order to augment the anatomical visualization of percutaneous ultrasound images, a model of the spine can be registered and overlaid on the iUS images. This type of registration is referred to as a model-based registration. Second, validation performed on human/animal data provides a more realistic scenario for experimentation, often resulting in a less accurate registration than with plastic phantom data. We report the type of data and the anatomy on which the validation was performed for each study. Third, because iUS images vary significantly from percutaneous to open-back surgery, it is worth considering the type of surgery in which the registration has been applied. In some cases, prior knowledge about the specificity of the iUS images can be used during the registration. For example, in open-back surgery images, depth gain loss is negligible due to good ultrasound propagation through the saline solution; on the other hand, percutaneous images may require depth intensity compensation of the ultrasound signal passing through different tissues. This is particularly important when imaging subjects with high body mass index. Fourth, the accuracy of the registration is reported when available. Note that it is not always possible to obtain a ground truth registration transform to assess the registration quality, especially when dealing with clinical data (i.e., human in vivo). In this case, the accuracy is assessed against a silver standard registration

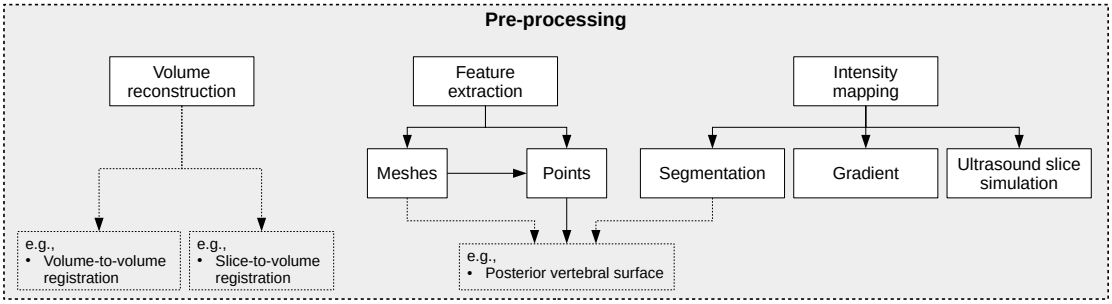

Figure 4: The pre-processing block involves volume reconstruction, feature extraction and intensity mapping. Dotted boxes represent use case examples.

that is obtained using metric evaluation, several repetitions or manual retrospective registration. These numbers are indicated by a '$*$' symbol and used to assess the registration in the absence of the ground truth transform. Finally, the computation time of the registration is reported when available. The computation time includes the registration time and the pre-processing time without including the time required for iUS acquisition and volume reconstruction, if applicable. Note that over 20 years, hardware computational performance has significantly increased; in addition, some reported works may include non-optimized code, which can render the computation time misleading. However, the computation time information as reported in Table 1 provides an indicator on *how iUS-based spinal navigation evolved in practice* and *how timing constraints were addressed in the reviewed papers.*

3. Image pre-processing

Before the registration, the data are prepared to enable the computations during the registration step. Depending on the registration method considered (described below in Section 5), three types of data pre-processing can be required (see Fig. 4): volume reconstruction, feature extraction and intensity mapping. Note that the pre-processing step are not mutually exclusive and some registration approaches require more than one pre-processing step. Pre-processing can have a significant impact on the registration time and quality. In this section, we focus our analysis on intra-operative pre-processing, as the timing frame during surgery is more critical.

3.1. Volume reconstruction

Commercial CT systems enable 3D reconstruction of volumes from the CT scans so that the CT volume is available shortly after the pre-operative scan session. This is not the case for most iUS-based navigation systems, where the acquisition consists of a sequence of tracked 2D ultrasound slices in which the position and orientation of each frame are known. A volume reconstruction is required to transform the 2D acquisition slices into a 3D compact volume (Solberg et al., 2007). Note that motorized ultrasound probes or 3D ultrasound probes that use a 2D-transducer-array to obtain real-time 3D volume acquisitions can be used. However, the restricted field of view of the imaged volume often requires a sweep to capture multiple volumes. A volume reconstruction needs to be performed by compounding the volumes of the sweep.

Because the iUS images are spatially tracked, the features extracted from each individual frame, such as vertebral surface points, form a 3D structure without the need for a volume reconstruction step. Therefore, most feature-based registration techniques do not require a volume reconstruction step. Considering image-based registration techniques, two types of approaches have been employed: volume-to-volume (i.e., 3D-3D) registration and slice-to-volume (i.e., 2D-3D) registration. When referring to volume-to-volume registration, the reconstructed volumes are compact, meaning that an intensity value is assigned to each voxel during the reconstruction. This approach is the most popular technique in image-based registrations as more information is contained in the volumes being registered. In general, slice-to-volume registration techniques are used when one of the imaging modalities yields 2D images, such as ultrasound imaging or radiography.

Table 1: Summary of ultrasound to CT registration methods.

Reference	Registration type	Validation	Anatomy	Surgery type	Accuracy TRE (mm)	Time	Pre-processing	Initialization	Registration
							Metrics		
Tonetti et al. (1998)	Rigid CT–iUS	Human cadaver	S1 to S2	Open	2.57	> 20 min	surface	manual	feature-based
							StealthStation point-based reg.		
Herring et al. (1998)	Rigid CT–iUS	Plastic phantom	L2	Open	N.A.	N.A.	surface	manual	feature-based
							ICP-based RMS point distance		
Ionescu et al. (1999)	Rigid CT–iUS	Plastic phantom	N.A.	Percut.	1.7*	N.A.	surface	manual	feature-based
							Graph-based RMS point distance		
Muratore et al. (2002)	Rigid CT–iUS	Plastic phantom	L1 to L3	Open	1.33–2.81	> 120 s	surface	manual	feature-based
							ICP-based RMS point distance		
Brendel et al. (2002)	Rigid CT–iUS	Human ex vivo	Lumbar	Open	N.A.	5-15 s	volume	manual	image-based
							Mean of iUS intensity		
Moulder et al. (2003)	Rigid CT–iUS	Plastic phantom	L4	Percut.	1.42	N.A.		manual	feature-based
							A-mode iUS, restricted surface matching		
Winter et al. (2008)	Rigid CT–iUS	Human in vivo	L2 to L5	Open	N.A.	5 s	volume intensity-mapping	manual	image-based
							Mean of iUS intensity		
Talib et al. (2011)	Rigid CT-iUS	Plastic phantom	L4	Percut.	1.29	< 1 s†	surface	manual	feature-based
							Information filtering		
Yan et al. (2012b)	Rigid CT–iUS	Porcine cadaver	T15 to L6	Open	1.65	164 s	volume, surface	manual	image-based
							Normalized cross-correlation		
Yan et al. (2012a)	Rigid CT–iUS	Porcine cadaver	T15 to L6	Open	1.48	116 s	surface	manual	image-based
							Normalized cross-correlation		
Gill et al. (2012)	Group-wise CT–iUS	Sheep cadaver	L3 to L5	Percut.	0.62–2.26	43 min	volume, intensity-mapping	manual	image-based
							Correlation Ratio + biomechanical model		
Lang et al. (2012)	Group-wise CT–iUS	Lamb cadaver	Lumbar	Percut.	1.61–1.89*	15–30 min	volume, intensity-mapping	manual	image-based
							Linear correlation of linear combination + speckle traking		
Rasoulian et al. (2012a)	Group-wise CT–iUS	Sheep cadaver	L1 to L5	Percut.	2.2	29 min	surface	manual	feature-based
							Unscented Kalman filte + biomechanical model		
Nagpal et al. (2015)	Group-wise CT–iUS	Human in vivo	L1 to L5	Percut.	0.71–1.70*	50–185 s	volume, surface	constrained	feature-based image-based
							Coherent Point Drift and mutual information		
Koo and Kwok (2016b,a)	Rigid CT/MR–iUS	Porcine cadaver	L2 to L6	Percut.	2.18	100 s	volume, surface	manual	image-based
							Normalized cross-correlation		
Behnami et al. (2016)	Model-based Model-iUS	Human in vivo	Lumbar	Percut.	2.1*	N.A.	volume, surface	constrained	feature-based
							Shape + pose model registration		
Echeverría et al. (2016)	Rigid CT-iUS	Plastic phantom	Lumbar	Open	0.76	N.A.	surface	automated	feature-based
							ICP-based RMS point distance and unscented Kalman filtering		
Chen et al. (2016)	Rigid CT-iUS	Human in vivo	L2 to L4	Percut.	2.3*	N.A.	intensity-mapping	automated	image-based
							Orientation code mutual information		
Ma et al. (2017)	Rigid CT–iUS	Sheep cadaver	Lumbar	Percut.	2.41	N.A.	surface	manual	feature-based
							Manual location of iUS landmarks		
Zettinig et al. (2017)	Deformable CT–iUS + Rigid iUS–iUS	Plastic phantom	L3/L4	Percut.	1.36	N.A.	volume intensity-mapping	constrained	image-based
							Linear correlation of linear combination		
Behnami et al. (2017)	Model-based Model–MR–iUS	Human in vivo	L1 to L5	Percut.	2.62–4.20*	8.1 min	surface	constrained	feature-based
							Shape + pose + scale model registration		
De Silva et al. (2018)	Rigid MR-iUS + Rigid iUS-iUS	Human cadaver	lumbar	Percut.	3.0	N.A.	volume	automated	image-based
							Linear correlation of linear combination + Normalized cross-correlation		
Gueziri et al. (2019)	Rigid CT-iUS	Porcine cadaver	L1 to L6	Open	1.48	11 s‡	volume, surface intensity-mapping	constrained	image-based
							Gradient orientation alignment		
Chan et al. (2020)	Rigid CT-iUS	Plastic phantom	T5 to T8	Open	1.2	16.2 s	volume	constrained	image-based
							Not specified		

(∗) No gold standard registration available, (†) Does not include segmentation time of iUS images, (‡) Including volume reconstruction time
Manual: Requires manual initial registration, Surface: Requires bone surface extraction on iUS images
Feature: Feature-based registration, Intensity: Intensity-based registration

Because the relationship between the spatial positions of the iUS slices is fixed, the acquisition frames can be processed as a rigid body during registration. A few papers reported the successful use of slice-to-volume registration applied to CT-to-iUS vertebra registration (Penney et al., 2006; Yan et al., 2012a; Chen et al., 2016).

It is also possible to create a sparse volume by compounding the images, in which in-between slice voxels are not assigned intensity values. During the registration, only voxels that have been assigned an intensity value in the sparse volume are used. This can be achieved by using a mask (Gueziri et al., 2019). While volume compounding is less computationally expensive than volume reconstruction, the procedure introduces intra-operative computation time.

3.2. Feature extraction

In this work, the term *feature* refers to specific anatomical and/or image characteristics that are spatially defined in the patient space. The goal of feature extraction is to provide the coordinates of 3D spatial anatomical structures that can be identified on both modalities and used for registration. During surgery, the features can be collected using a tracked pointer in invasive surgery, using a tracked needle in minimally invasive surgery or using a time of flight device (e.g., A-mode ultrasound) in non-invasive surgery (Amstutz et al., 2003). In CT/MR-to-iUS image registration, the features need to be extracted from images then converted into 3D spatial coordinates.

Most spinal fusion surgeries are performed using a posterior approach, with the patient placed in prone position and the vertebrae accessed via a dorsal opening. In this case, the iUS acquisition needs to be performed with the probe positioned at the back of the patient and oriented approximately normal to the coronal plane. Because of the acoustic shadow produced by bony tissues, only the posterior surface of the vertebrae is visible on the iUS images. The posterior surface of the vertebra is a good candidate feature for rigid registration, as the vertebra forms a rigid structure. Note that in some cases, an anterior surgical approach can be adopted for lumbar or cervical level fusion in order to avoid prior surgery areas, to access intervertebral disks or to add lordosis to the spine. However, no papers in this review reported the feasibility of using iUS-based navigation in an anterior approach spine procedure.

On the CT image, the density of bone tissues correlates with the CT intensity which lies between 140 to 260 Hounsfield units (HU) (Yan et al., 2011; Sugano, 2003; Winter et al., 2008). The posterior surface of the vertebrae can be obtained by ray tracing a line going from posterior to anterior, in which the surface location corresponds to the first occurrence of voxels above a given threshold, typically 150 HU (Brendel et al., 2002, 2005; Winter et al., 2008, 2009; Yan et al., 2011, 2012b,a; Gueziri et al., 2019). The approach yields satisfactory results to extract the posterior vertebral surface. Since this step is performed pre-operatively, the computation time to achieve the task is not critical. On pre-operative MR images, the full vertebra can be segmented using manual or semi-automatic approaches and the posterior surface is obtained using ray tracing (Koo and Kwok, 2016a).

Extraction of the vertebral surface on iUS images is challenging. Many approaches have been proposed to segment the bone surface on ultrasound images. Interested readers are referred to a review on the topic (Hacihaliloglu, 2017). Among the proposed approaches for bone-tissue region segmentation, some considered using hyperechoic intensity and shadow indicators (Kowal et al., 2007; Foroughi et al., 2007), image local phase information (Hacihaliloglu et al., 2009, 2013b,a; Hacihaliloglu et al., 2014; Jia et al., 2016), random forests (Berton et al., 2016), eigenanalysis of the Hessian matrix (Fanti et al., 2018), beamforming (Zhuang et al., 2019) or more recently using convolutional neural networks (CNN) (Salehi et al., 2017; Baka et al., 2017; Alsinan et al., 2019). Because the segmentation of iUS is performed intra-operatively, the computation time needs to be reduced as much as possible. More importantly, the accuracy of bone segmentation is crucial for feature-based registration approaches, as the location of the surface affects the final registration quality.

3.3. Intensity mapping

Unlike feature extraction where the output is a set of spatial coordinates for an anatomical structure, the output of the intensity mapping is an image in which the intensities of some specific anatomical structures are highlighted. Intensity mapping is used in image-based registration approaches to allow metric comparison

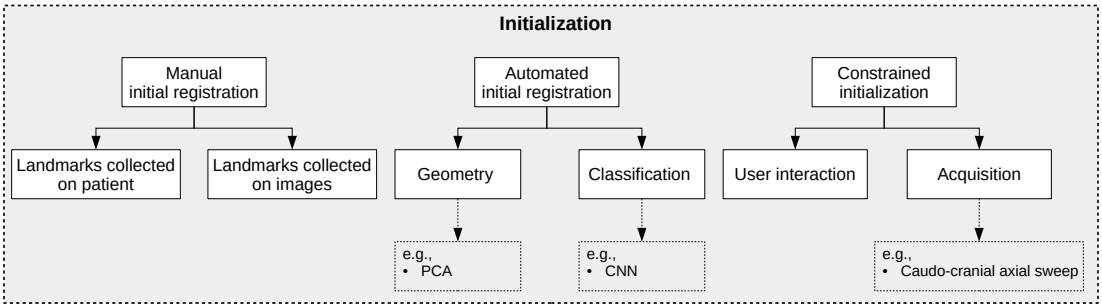

Figure 5: The initialization block involves manual, automated and constrained initialization techniques. Dotted boxes represent use case examples.

between the information represented in the pre-operative CT/MR images and the information represented in the iUS images. A simple technique consists in segmenting the posterior vertebral surface, on both CT/MR and iUS images and use the binary segmented image in the registration step. In this context, the feature extraction step is seen as an intensity mapping method. This approach has been used in (Yan et al., 2011, 2012b,a; Koo and Kwok, 2016a,b; Gueziri and Collins, 2019; Gueziri et al., 2019), where the binary segmented images of posterior vertebral surface on both iUS and CT images were registered. The vertebral surface on iUS images was obtained using a simple ray-tracing approach. It is not always necessary to segment the iUS images. Instead of using binary images, the contrast between the vertebral surface and the surrounding tissue can be enhanced. Winter et al. (2008, 2009) proposed to use an adaptive depth gain compensation filter to enhance bone-tissue interface appearance on iUS images. Similarly, the enhanced iUS images were registered to a pre-segmented vertebral surface on CT images. Using low-level filtering, Penney et al. (2006) converted both CT and iUS images into probability density maps of bone structure representation. Others (Gill et al., 2009a, 2012; Lang et al., 2012; Zettinig et al., 2017) mapped the CT intensities to simulate ultrasound-like images to be compared with the real iUS images. In order to use an image-based phase correlation metric, Hacihaliloglu et al. (2013b) first preprocessed both CT and iUS images with a local phase filtering. Then, the filtered images were projected into Radon transform space.

4. Initial registration

Initialization of the starting position for registration is a common problem in many medical applications. The goal of the initial registration is not to achieve a highly accurate patient registration. Rather, it is to bring the patient position sufficiently close to the real solution without causing significant disruption of the clinical workflow. This is particularly true for spine registration where the anatomical similarity of the vertebrae may cause the registration to align images of the wrong vertebral level. Despite its importance, the issue has received little attention as most of the papers reviewed assume a *reasonable initial misalignment*, usually comprised within ± 10 mm of translation and $\pm 10^\circ$ of rotation error. Figure 5 shows the different types of initialization approaches used in spine surgery.

4.1. Manual initialization

Although time-consuming, manual registration is the most used initialization technique in spine intervention. It is already established in the clinic. In the absence of an automatic patient alignment method, it is considered to be the standard registration method during surgery. The procedure consists in collecting pairs of landmarks in both modalities. Then, a rigid-body registration approach is applied to minimize the distance between each pair of points. The technique only requires a few landmarks, typically 4 to 7 points. The landmarks can be collected directly on the patient using a tracked pointer or identified on the iUS images.

4.2. Constrained initialization

An alternative approach for initialization is to constrain the iUS acquisition such that the real solution can be approximated a priori. This can be formulated as a set of assumptions and requirements that need to be met during iUS acquisition. In this context, Nagpal et al. (2015) used the assumption that the number of vertebrae imaged with the ultrasound probe is the same as that present on the pre-operative CT. Then, the two volumes are aligned relying on their center of gravity and using image-based mutual information registration. However, this does not account for large orientation misalignments, such as left-right and superior-inferior image flips. In addition to the same number of vertebrae, Gueziri and Collins (2019) and Gueziri et al. (2019) proposed to use a constrained iUS acquisition protocol to guarantee a roughly correct orientation. The protocol consists of a single sweep starting from inferior up to the superior part of the spine centered on the spine mid-line. The initial registration is achieved by aligning the iUS probe trajectory with the known caudo-cranial direction of the pre-operative images. Based on the assumption that pre-operative images are acquired in supine position whereas iUS images are acquired in prone position, Behnami et al. (2016, 2017) used an interactive registration that involves a single-click interaction to approximately align the center of gravity of the L3 vertebra. Using a robotically steered iUS probe, Zettinig et al. (2017) also leveraged the user interaction to roughly initialize the translation component of the registration. The rotation component was based on the assumption of prone position with a transverse iUS acquisition.

4.3. Automated initialization

In the context of automatic initialization of the registration transform, Echeverría et al. (2016) proposed to use principal component analysis (PCA) to align the principal axes of the vertebral posterior surface points. The method is motivated by the geometry of the point distribution along the anterio-posterior (on the spinous process) and the left-right/superior-inferior axes (on the transverse and articular processes). Different iUS acquisition scenarios were evaluated, in which the posterior surface points were collected. Successful registrations were achieved when sufficient points are present on the iUS data. However, the method fails to provide a good initial alignment in the presence of outlier points, i.e., those that belong to neighboring vertebrae, which reflects a more realistic acquisition case. Using image classification, Chen et al. (2016) proposed to train a CNN model based on CaffeNet (Jia et al., 2014) to recognize five pre-established iUS scan scenarios for L2 to L4 vertebrae. Prior to the registration, the iUS images are classified into the corresponding scan scenario and a pre-defined initial transformation is applied. Among the 100 iUS images tested, 91.09 % were classified correctly. Unlike the PCA-based approach (Echeverría et al., 2016), the method has the advantage of not relying on an extracted feature that may introduce additional noise. However, the pre-defined initial transformation associated with each scenario introduces a strong assumption about the patient anatomy, which may not be always valid. In the context of 2D-3D registration, De Silva et al. (2018) used an image classification method to initialize the position of the iUS slices in the 3D ultrasound volume. Once the 3D volume of the target vertebra was acquired, axial and sagittal slices were sampled to build a dictionary associating the slices with their corresponding positions in the volume. For each sampled slice, a Haar-like feature vector (Viola and Jones, 2004) was extracted and stored. Prior to registration, the Haar-like feature vector of the current 2D iUS image is extracted and compared to the dictionary feature vectors using normalized cross-correlation. The initial alignment is achieved by assigning the position of the most resembling slice in the dictionary to the current image, i.e., with the highest correlation. Although the method does not directly address the problem of CT/MR-to-iUS initialization, results showed good application to slice-to-volume initialization for patient monitoring.

5. Registration

Registration is the main component of patient alignment. In this section, we discuss feature-based and image-based registration approaches (see Fig. 6).

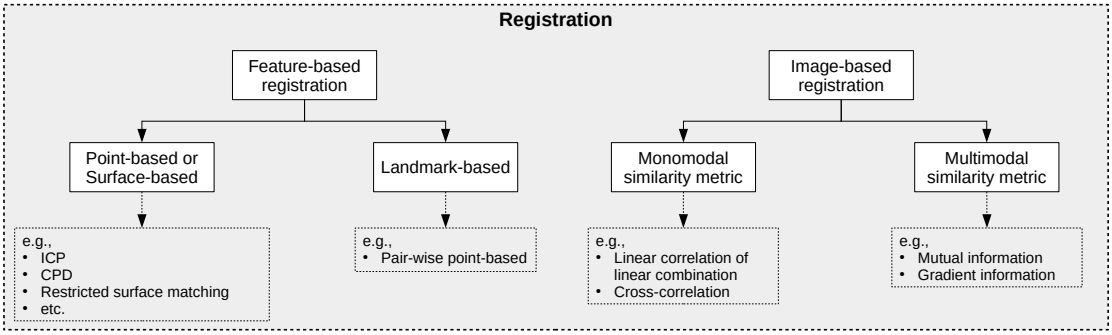

Figure 6: The registration block involves feature-based and image-based registration techniques. Dotted boxes represent use case examples.

5.1. Feature-based registration

Feature-based registration, also referred to as point- or surface-based registration, aims at registering two sets of spatial features extracted from the pre-operative CT/MR and the iUS images. In spine registration, the features consist of a set of points lying on the posterior surface of the vertebra that is visible on iUS images. The region from which the points are extracted includes the apex of the spinous process, the laminae, the posterior part of the transverse processes, the inferior articular processes and a small area on the posterior part of the vertebral body. When the corresponding pairs of points are known on each modality, the registration problem can be solved using a landmark-based registration approach. In this context, Ungi et al. (2013) evaluated the feasibility of pair-wise point-based registration in pedicle screw fixation, by manually identifying intra-operatively the posterior-most portions of articular processes on tracked iUS images. The registration was achieved successfully with a TRE of 1.28 mm. Xie et al. (2020) employed skin-attached fiducials to register pre-operative MR images to patient space. Then, landmarks on the spinous process were identified on iUS images and used to correct for eventual misalignments. However, specific landmark identification on iUS images is not trivial, requiring the surgeon to be familiar with ultrasound imaging. In the general case, point correspondences are not available. The registration problem is formulated as an expectation-maximization algorithm that consists in optimizing some cost function that expresses the point sets alignment. The iterative closest points (ICP) (Besl and McKay, 1992) algorithm has been extensively used in this context.

Early work involving iUS-based navigation used manual segmentation of the posterior vertebral surface on iUS images (Tonetti et al., 1998). The procedure was time-consuming, $\sim$ 20 min for 40 images, and requires high expertise. Using morphological filtering to automatically extract the points from iUS images, Herring et al. (1998) studied the effect of point distribution on the registration quality. The points were sampled from different anatomical regions of the vertebra using a tracked pointer and registered to the points extracted from images of a non-tracked iUS probe. Phantom experimentation showed that points collected on the laminae surface and the apex of the spinous process yield the best results. Later, the work was extended by Muratore et al. (2002) to include an IGS navigation setup using a tracked iUS probe. Similar studies on the effect of point distribution were reported for manual landmark-based registration (Ershad et al., 2014) and surface-based registration with CT navigation (Wang and Song, 2013). Ionescu et al. (1999) used high-level feature segmentation to match candidate segments that yield the best CT-to-iUS image alignment. For each segment extracted on an iUS slice, a set of possible transformations is generated per slice. The final registration consists in retaining the best transform that minimizes the segment distances between all the iUS slices and the CT image. Results showed application to a single vertebra registration, but limited validation experiments preclude further conclusions.

Using A-mode ultrasound to extract surface points, Moulder et al. (2003) employed a *restricted surface matching* method (Bächler et al., 2001) that combines landmark-based and point-based approaches to align the vertebral surface points. In addition to the surface points, the method uses 3 to 5 known anatomical landmarks to guide the registration. Because the pair-wise correspondence of the landmarks was known a

priori, a penalty term was associated with landmark misalignment during registration. A-mode ultrasound was also employed for surface point extraction on tibia and femur in (Mozes et al., 2010) and on spinous process (Lou et al., 2010).

Barratt et al. (2006) proposed to optimize the iUS probe calibration parameters during the registration. The approach involves a four-step registration process: 1) perform a rigid surface-based registration, 2) remove outlier points and perform a rigid surface-based registration, 3) perform a rigid surface-based registration including the y-axis pixel scaling calibration parameter that corresponds to the probe depth, and 4) perform a rigid surface-based registration including all iUS calibration parameters. The method was successfully applied to femur and pelvis bone registration of human cadavers. One disadvantage of adjusting the calibration transform while registering is the risk of over correcting the calibration parameters in the case of mis-registration. Additionally, in order to cover all the necessary views for the calibration to be optimized, multiple translation positions and angular orientations need to be performed with the iUS probe during the acquisition. Vertebral surface points were manually segmented to avoid including feature extraction errors in the evaluation.

To deal with outlier points and errors related to feature extraction, different approaches have been investigated including Kalman filtering (Rasoulian et al., 2012a; Echeverría et al., 2016) and information filtering (Talib et al., 2011) for spine registration; as well as Gaussian mixture model sampling (Hacihaliloglu et al., 2012) for pelvis registration. Given already extracted surface points, the registration method proposed by Talib et al. (2011) allows for real-time iterative registration. The approach has been applied for incremental (frame-by-frame) correction of the registration during iUS data acquisition. Experiments on a plastic phantom of L4 showed good accuracy of 1.29 mm. Although the concept of incremental registration looks attractive, as it provides the surgeon with feedback on the quality of the acquisition, the method inherits the limitations of ICP registration including the sensitivity to the initial alignment.

Because the pre-operative images are usually acquired with the patient in supine position and the iUS scans are acquired with the patient in prone position, the spine curvature is subject to change between the two acquisitions. Aligning multiple vertebrae using a single rigid registration does not account for the spinal posture difference. In order to correct the spine curvature, Rasoulian et al. (2010, 2012a) proposed to perform a group-wise rigid registration of multiple vertebrae. First, each CT sub-volume containing a single vertebra is independently aligned to the corresponding iUS volume using a surface-based rigid registration. Then, the resulting transforms are applied to the entire CT volume using a regularization biomechanical model. The idea consists in using extra intervertebral points that act like a spring to prevent incoherent transformations. Experiments on a sheep cadaver showed the successful application of the method in the context of percutaneous spinal injections. A computation time of 29 min was reported, which significantly impacts the surgical workflow as increasing surgery duration is associated with multiple postoperative complication risks (Kim et al., 2014). Similarly, Nagpal et al. (2014, 2015) proposed a group-wise registration method based on the coherent point drift (CPD) algorithm (Myronenko and Song, 2010). To correct for spine curvature, extra intervertebral points were manually introduced to act as regularization constraints during the registration. The computation requires only 50–185 seconds, enabling applications in surgery.

Application of feature-based registration showed good results for CT/MR-to-iUS spine registration, overcoming issues related to image intensity differences at the cost of rendering the registration accuracy dependent on the feature extraction quality. Nevertheless, the vertebral posterior surface proved to be a valid anatomical landmark for registration. Experiments on animal and human cadavers reported a TRE ranging between 2.2 mm and 2.57 mm. For clinical data involving human in vivo experiments, in which the ground truth transform is not available, the registration is evaluated against a sub-optimal registration yielding an error ranging between 0.71 mm and 4.2 mm. Another advantage of the feature-based registration is that there is no need for iUS volume reconstruction. Features that are extracted from an iUS slice can be converted to 3D structures using its corresponding spatial position, reducing intra-operative processing time. The time required to extract surface points, whether this is done manually (several minutes) (Tonetti et al., 1998; Barratt et al., 2006; Ma et al., 2017), using an A-mode ultrasound probe (real-time) (Moulder et al., 2003; Mozes et al., 2010) or automatically (from seconds to minutes) (Herring et al., 1998; Ionescu et al., 1999; Muratore et al., 2002; Rasoulian et al., 2012a; Nagpal et al., 2015; Behnami et al., 2016, 2017), potentially impacts the surgical workflow.

5.2. Image-based registration

Image-based registration relies on the comparison of image intensities using an image intensity-based *similarity metric* to assess the alignment of pre-operative and intra-operative images. Similarity metrics derived from the sum of squared differences (SSD) (Ashburner and Friston, 1999; Friston et al., 1995; Hajnal et al., 1995; Woods et al., 1998) and cross-correlation (Cideciyan, 1995; Collins and Evans, 1997; Guimond et al., 2001; Hermosillo et al., 2002) are widely used in monomodal image registration. The general underlying assumption is that the same anatomical structure should have the same intensities when using SSD or a linear relationship when using cross-correlation (Oliveira and Tavares, 2014). In multimodal image registration, the intensities of the same anatomy may vary significantly from an imaging modality to another, e.g., in spine imaging bony structures appear as bright on CT images, gray on routine T2-weighted MR images and only the bone surface facing the probe's transducers appears on iUS images. Similarity metrics based on the previous assumptions would fail. In this context, image alignment can be assessed either by mapping the image intensities to a common intensity space, so that the assumption becomes valid, or by using a similarity metric that takes into account intensity differences.

For both CT and iUS images, Penney et al. (2006) computed the probability density function that a given voxel lies on a bone surface. Because the probability maps highlight the same anatomical structures, normalized cross-correlation was successfully used for pelvis and femur registration. Similar to the work proposed by Barratt et al. (2006), the depth parameter of iUS probe calibration was considered during the optimization of the rigid registration in order to correct for variations of the speed of sound. In the context of lumbar fusion open surgery, Yan et al. (2011, 2012b) successfully used cross-correlation to register binary segmented CT and iUS images. Later, a slice-to-volume version of the method was proposed to reduce intra-operative computation time related to iUS volume reconstruction (Yan et al., 2012a). The iUS images were segmented using a backward ray-tracing technique that exploits shadow artifacts produced by the bony vertebra structure. Because the registration is applied to binary images, the approach can be applied to different modalities and surgery types. For example, the approach was employed in a hierarchical registration framework to register percutaneous iUS images with CT images (Koo and Kwok, 2016b) and MR images (Koo and Kwok, 2016a).

To avoid intra-operative segmentation of ultrasound images, Brendel et al. (2002) and Winter et al. (2002) proposed to maximize the intensity sum of the points located at the posterior surface of the vertebra on CT images. This is motivated by the hyper-echoic response of the vertebral surface in iUS images. When images are aligned, the points located on the CT posterior surface should pass through bright voxels representing vertebral surface on iUS images. Because only the locations of CT vertebral surface points are used during the registration (not the CT intensities), the approach does not require intensity mapping pre-processing. Later, Winter et al. (2008) proposed to enhance the contrast of the vertebral surface on iUS images to improve the registration quality.

In the context of CT-to-iUS liver registration, Wein et al. (2008) proposed to use simulated ultrasound images computed from CT images. Considering a given iUS probe position, ultrasound-like penetration signals passing through the different tissues were calculated based on the CT intensities. The associated iUS image was then reconstructed. The simulated and the real iUS images were registered using a linear correlation of linear combination (LC^2) metric. The metric assesses the correlation between the iUS intensities and a linear combination of the reflection and ultrasound-simulated signals extracted from CT. Gill et al. (2012, 2009b) and Chen et al. (2010) employed this method to achieve multi-level vertebra registration for minimally invasive surgery. A biomechanical model based on intervertebral displacement, reaction forces and moments (Panjabi et al., 1976; Gardner-Morse et al., 1990; Desroches et al., 2007) was used to constrain non-realistic vertebral motion. The method achieved high registration accuracy with a reported TRE ranging from 0.62 mm to 2.26 mm on a sheep cadaver. However, the computation time of 43 min is too slow to be considered in a clinical workflow. The LC^2 metric was also used in (Zettinig et al., 2017) and (Lang et al., 2012). Zettinig et al. (2017) used a deformable free-form transform to initialize the CT-to-iUS registration (Modat et al., 2010). Then, the iUS probe motion is tracked to monitor patient positioning using cross-correlation in an iUS to iUS registration framework. Lang et al. (2012) proposed a speckle-based iUS probe tracking method. To correct for positional drifts induced by speckle-tracked ultrasound, CT spine images

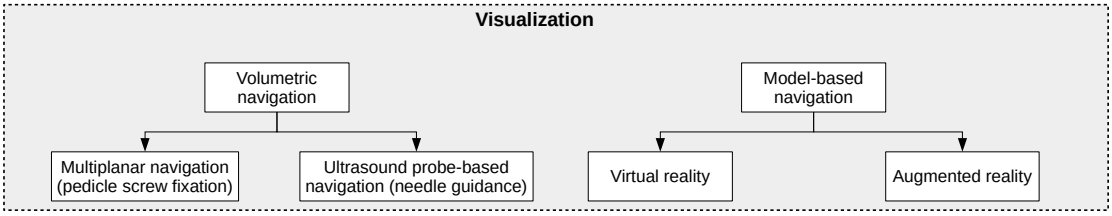

Figure 7: The visualization block involves volumetric and model-based navigation techniques.

are registered to iUS images using the framework proposed by Gill et al. (2012). The method demonstrates the feasibility of sensorless ultrasound navigation by improving iUS tracking accuracy. However, the initial position of the iUS volume needs to be specified, which in the study is provided using an optical tracking device.

Hacihaliloglu et al. (2013b) used a phase correlation metric to register CT and iUS pelvis images. First, local phase bone images were extracted using a log-Gabor filter then projected into a Radon space. The registration transform was determined using a two-step integration procedure. An average surface registration error of 0.78 mm was achieved on clinical data of two patient pelvis images.

The use of multimodal metrics can obviate the need for intensity mapping pre-processing. Mutual information (MI) and its derived metrics have been extensively used in multimodal registrations involving ultrasound imaging (Shekhar and Zagrodsky, 2002; Walimbe et al., 2003; Leroy et al., 2004; Wein et al., 2005; Ji et al., 2008; Rivaz et al., 2014). In the context of CT-to-iUS spine registration, MI was applied by Nagpal et al. (2015) to initialize the registration transform. Chen et al. (2016) combined gradient orientation and mutual information to achieve slice-to-volume registration. Two-dimensional gradients of CT and iUS slices are used to encode orientation information. Using information theory, the similarity metric is estimated using the entropy of the probability density function of the orientation codes. A gradient orientation metric was also proposed to register segmented CT and iUS vertebral surface images (Gueziri et al., 2019). In contrast to SSD and cross-correlation where the intensities of anatomical regions are being compared, gradient-based metrics rely on the contrast induced at anatomical boundaries. Validations on a porcine cadaver achieved a TRE of 1.48 mm in 11 seconds of computation, which is clinically acceptable for spine surgery. Recently, Chan et al. (2020) evaluated the accuracy of a multi-camera IGS system on a thoracic spine phantom. Positional and angular errors were reported to be $1.2\,\text{mm} \pm 0.5\,\text{mm}$ and $2.2^\circ \pm 2.0^\circ$ in $\sim 16\,\text{s}$ of computation. The alignment relies on an image-based Gaussian pyramid registration approach. Unfortunately, technical details of the similarity metric employed have not provided.

6. Visualization

A common concern in IGS navigation is the assessment of the spatial positioning of the instrument with respect to the patient pre-operative images. The way instruments are displayed to the surgeon affects the efficiency with which the navigation is performed. In fusion surgery, the navigation helps to identify the entry point and trajectory of the pedicle screw. The visualization needs to display internal bony anatomical information including the pedicle walls and the vertebral body. On the other hand, in spine injection, the needle is inserted through the intervertebral gap to reach the injection target location, e.g., facet joint or epidural space. The emphasis of the visualization is focused on external bone anatomy to navigate through soft tissue. In spine interventions, we identified two main categories for the visualization of instrument navigation (see Fig. 7): volumetric navigation in which the instrument is located according to the pre-operative 2D slices, and model-based navigation in which the instrument is visualized with respect to a 3D display of the spine model.

6.1. Volumetric navigation

Most spinal IGS systems use multiplanar reconstruction of pre- or intra-operative CT or MR images for navigation. Orthogonal planes, characterized by the axial, sagittal and coronal views, are commonly used

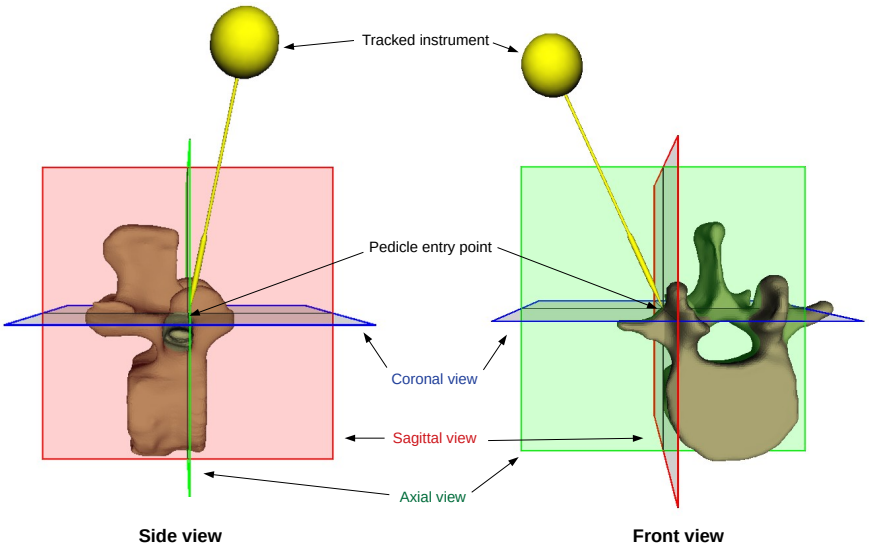

(a)

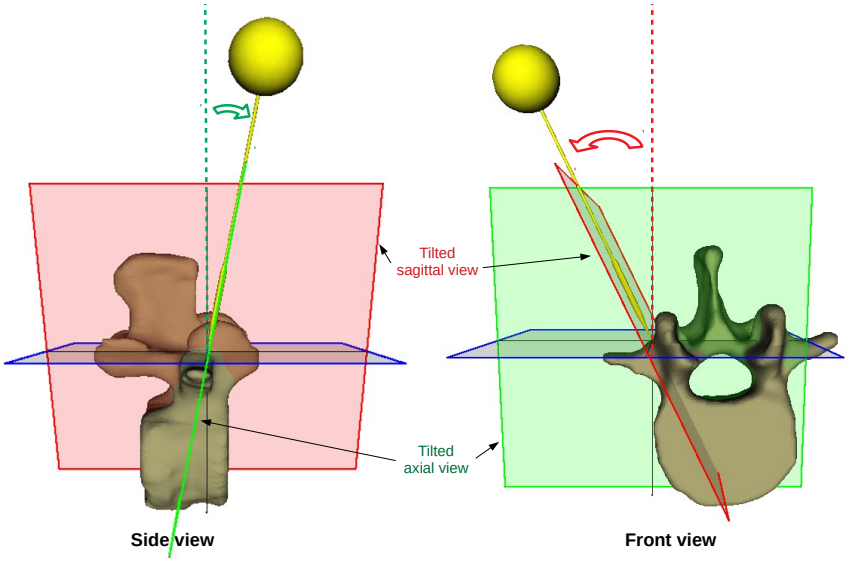

(b)

Figure 8: Navigation using multiplanar reconstruction volume: (a) orthogonal MPR planes, and (b) tilted MPR planes.

to explore volumetric data. The advantage of multiplanar reconstruction is to provide reconstructed slices in any arbitrary orientation. This is used in pedicle screw fixation where axial and sagittal views are tilted so that their angular orientation is aligned with the tracked instrument orientation (see Fig. 8). Note that the coronal view is not tilted. It is used to indicate the pedicle entry point and to assess the spine curvature in the case of spine deformity correction. During navigation, a projection of the pedicle screw is used to augment the axial and sagittal views by highlighting the predicted trajectory prior to implantation. This allows viewing the anatomy that will be traversed by the pedicle screw to prevent breaches (see Fig. 9).

Another use of multiplanar reconstruction volumetric navigation is to leverage the iUS probe orientation to display the corresponding view in other modalities, as reported by Liu et al. (2018) for transforaminal puncture. Once manual registration was established between intra-operative CT, pre-operative MR and

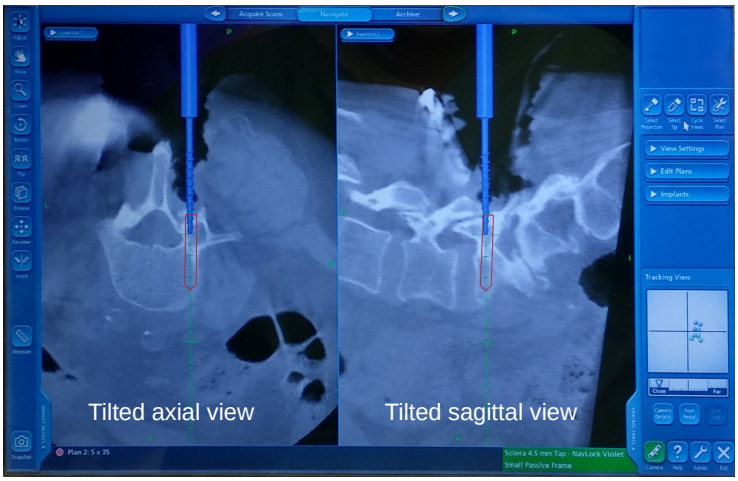

Figure 9: Example of navigation using multiplanar reconstruction and tilted views: a virtual model of the tracked instrument is shown in blue and a cross-section of the planned screw insertion is shown in red.

patient space, the puncture target was identified and a tracked iUS probe was used to obtain arbitrarily oriented slices. The corresponding reformatted CT and MR slices were displayed on the screen to provide anatomical information during needle insertion. Percutaneous spinal needle insertion is commonly achieved using ultrasound guidance. This approach benefits from CT and MR enhanced anatomy imaging while preserving the clinician's standard practice in ultrasound guidance.

6.2. Model-based navigation

Navigation using multiplanar reconstruction 2D views is not trivial as it requires a high knowledge of the spine anatomy and a considerable effort to mentally map hand-eye coordination with the view. Alternative approaches consist in augmenting navigation images with a 3D model of the spine. While CT images provide good visualization of the spine anatomy, ultrasound images are more difficult to interpret and may highly benefit from visual augmentation. This is the case in the context of spinal needle insertion. In most cases, the CT images of the patient are not available and the clinician relies solely on ultrasound images. The use of *anatomical atlases* has been considered as an alternative option in the absence of pre-operative CT images for femur and pelvis registration (Talib et al., 2005; Tang and Ellis, 2005; Barratt et al., 2008; Foroughi et al., 2008), MR intervertebral disc segmentation (Michopoulou et al., 2009), scoliosis assessment (Boisvert et al., 2008) and needle guidance (Khallaghi et al., 2010, 2011; Rasoulian et al., 2012b, 2013b,a). Atlas-based (or model-based) registration relies on the use of a statistical model computed from several patient scans. The model encodes the mean shape and the statistical variability of the vertebrae across the anatomy of all the patients. During navigation, a model-to-iUS registration is performed so that the statistical model is aligned with the specific anatomy of the patient being scanned while simultaneously updating the model parameters to tailor it to the patient's anatomy.

Virtual reality (VR) can augment the 2D iUS images with the visualization of a patient-specific 3D spine model for needle guidance as proposed by Moore et al. (2009); Rasoulian et al. (2015); Seitel et al. (2016). Rasoulian et al. (2014, 2015) used an electromagnetic tracking system to track the iUS probe and the injection needle. Posterior surface probability maps are extracted from iUS images and used to register the 3D spine model shape and pose. Then, the 3D virtual models of the iUS image and the needle are displayed relative to the spine model so that the clinician can navigate using the VR canvas. Behnami et al. (2016) extended the method by jointly registering the model to the patient's CT scan while aligning the model with the iUS images. Later, the approach was adapted to register the model to MR and iUS images (Behnami et al., 2017).

Brudfors et al. (2015) proposed to augment the 2D iUS view with axial and sagittal cross-sections of

the model contour to provide the clinician with key anatomical information for epidural injection. Once the desired vertebral level identified, ultrasound volumes were collected using a 3D probe. The proposed optimized implementation allows for continuous registration of the model with the iUS volumes providing automatic updates of the model shape and pose during navigation. A similar visualization technique was proposed by Tiouririne et al. (2017) where a hand-held ultrasound probe was used to highlight neuraxial landmarks for needle guidance. The model was registered using affine transformation of model surface points.

For needle guidance in facet joint injections, Ungi et al. (2012) used a VR environment in which ultrasound slices are spatially positioned in the view. Each ultrasound slice consists of a snapshot captured by the clinician before the needle insertion. The entry point and the target are then defined by specifying two points on the recorded snapshots and the needle trajectory is defined as the line connecting the two points. Navigation is achieved by simultaneously displaying two views: a "*bull's-eye view*" in which the virtual camera position is co-linear with the two points, and a "*progress view*" similar to a sagittal view used for monitoring the needle insertion depth. The study reported that better hand-eye coordination was achieved using the proposed views than using the standard ultrasound-guided needle insertion procedure.

Another use of ultrasound in interventional spine procedures is the identification of vertebral levels. Lumbar puncture and injection sites, often located in the L2/3, L3/4 and L4/5 intervertebral spaces, can be identified by palpation of the spine with a reported success rate of 30–63 % (Furness et al., 2002; Hayes et al., 2014; Whitty et al., 2008; Lee et al., 2011; Stiffler et al., 2007). The procedure shows a variability in the results for pregnant patients, for adults and children patients and in patients with a high BMI and a pathological or a surgical history. The same studies reported an improvement in the success rate to 71-73 % when using ultrasound imaging. Automatic labeling of vertebral levels for percutaneous needle insertion has been considered using panoramic parasagittal ultrasound views constructed by image stitching (Kerby et al., 2008). Starting from the coccyx and moving cephalad along the lumbar spine, vertebral levels are identified by counting the number of peaks detected in parabolic curves fitted to the panoramic image. Rafii-Tari et al. (2011, 2015) proposed to use a camera mounted on the probe to allow positional tracking and facilitating the panoramic view reconstruction. Using parasagittal ultrasound images, Hetherington et al. (2017b) proposed to track peaks of the curves produced by the laminae during the acquisition. The vertebral levels are identified by detecting new peaks on the image. An alternative approach using a CNN-based classification was proposed by Hetherington et al. (2017a). Axial images were classified into "gap" and "bone" classes representing intervertebral and vertebral spaces, respectively. Starting from the coccyx, a state machine was used to identify the vertebral level by incremental counting.

Virtual augmentation of ultrasound images without the use of preoperative 3D models has been investigated. This type of approaches focuses on identifying relevant anatomical landmarks directly from the ultrasound images, without the need for additional model-based registration steps. Thus, the risk of errors related to the registration is reduced. Such approaches have been investigated for the identification of neuraxial landmarks in epidural injection guidance (Pesteie et al., 2018; Oh et al., 2019) and spinous process and laminae landmarks in scoliosis assessment (Brignol et al., 2020).

The use of 3D spine models during navigation provides an intuitive interpretation of the instrument's position with respect to spine anatomy. However, the focus of the surgeon's attention is constantly shifting between the screen in which the virtual scene is displayed and the surgical site, affecting the surgical performance and efficiency (Peters and Cleary, 2008). To address this issue, augmented reality (AR) techniques produce a composite display in which a virtual scene can be overlaid on the real image, providing an in situ visualization of the spine model. In spine-related applications, the use of AR-based visualization has been investigated for vertebral level identification (Al-Deen Ashab et al., 2013), pedicle screw fixation using integral videography (Ma et al., 2017), ImmersiveTouch (ImmersiveTouch inc, Chicago, IL, USA) simulator (Luciano et al., 2011) and see-through video (Elmi-Terander et al., 2016); as well as for vertebroplasty (Wu et al., 2014) using camera-projection, spinal injection (Fritz et al., 2013) and more recently tumor resection (Carl et al., 2019b) using image overlay. Interested readers are referred to the survey on AR utilization in orthopedic surgery (Ma et al., 2018; Alaraj et al., 2013).

7. Validation

Cleary et al. (2000) presented a report discussing technical requirements for image-guided spine procedures based on the consensus from about 70 experts, in which particular concerns were expressed regarding the validation of image-guided intervention systems. The report identified four criteria that need to be considered during validation:

- *accuracy* is the degree of exactitude with which the instrument is located with respect to the patient anatomy or images,
- *robustness* is the stability with which the registration is achieved,
- *reliability* is the ability of the system to reproduce the results, and
- *usability* represents the clinical utility of the system in terms of time efficiency, user interaction, surgical value, etc.

In this section, we identify patterns commonly used in the literature during spinal IGS and we detail the implication of each criterion in the validation process.

7.1. Accuracy

In what follows, we focus our discussion on the assessment of the registration quality. Therefore, we assume that the information provided by the equipment (i.e., tracker and ultrasound) and the calibration procedure is exact. We also assume that the DRO was not displaced after the registration has been achieved, insuring the error measurements are due to the registration process only. In pedicle screw fixation, post-operative imaging is the clinical method for the inspection and confirmation of intrapedicular insertions and breaches (Carl et al., 1997; Girardi et al., 1999; Liu et al., 2005; Kaneyama et al., 2014). Post-operative implanted screws are compared to the pre-operative insertion planning to assess how successfully the surgery followed the planning. The advantage is that the accuracy at which the position of the inserted screws is evaluated depends on the image quality and the operator, reducing error sources such as tracking information or DRO displacement. On the other hand, such validation extends the evaluation of the IGS system to include the performance of the surgeon, e.g., deliberate compensations for small inaccuracies.

In the case where the post-operative images are not available, the registration transform, $\mathbf{T}$, obtained using CT/MR-to-iUS images needs to be compared to a reference transform, i.e., a *gold standard transform* representing the ground truth $\mathbf{T}_{\text{gt}}$. When possible, the gold standard transform should be obtained using implanted fiducials as recommended by Cleary et al. (2000). The procedure involves rigidly inserting markers in the bone tissue (usually, the vertebral body, to avoid interfering with iUS acquisitions) so that each marker can be accurately identified in both pre-operative images and using a tracked pointer. A set of target points is identified on the pre-operative image space and then transformed into the patient space using $\mathbf{T}$ and $\mathbf{T}_{\text{gt}}$. The average distance between the pair-wise transformed points represents the TRE. This validation metric has been used in many papers (Tonetti et al., 1998; Muratore et al., 2002; Moulder et al., 2003; Talib et al., 2011; Yan et al., 2012b,a; Gill et al., 2012; Rasoulian et al., 2012a; Koo and Kwok, 2016b; Echeverría et al., 2016; Ma et al., 2018; Zettinig et al., 2017; De Silva et al., 2018; Gueziri et al., 2019).

In the absence of the gold standard transform, for example when fiducials cannot be implanted, two approaches have been considered. The first approach consists in establishing a reference transform using manual registration techniques, thus generating a *silver standard transform* representing a suboptimal ground truth $\mathbf{T}^*_{\text{gt}}$. For example, the silver standard transform can be obtained by using landmarks manually identified in pre- and intra-operative images (Hacihaliloglu et al., 2013b; Nagpal et al., 2015; Behnami et al., 2017) or by averaging the best registration results and manual corrections (Winter et al., 2002; Brendel et al., 2005; Lang et al., 2012). The inconvenience of the latter method is that it measures convergence of the registration instead of the accuracy. Then, a proxy TRE is computed using the silver standard transform $\mathbf{T}^*_{\text{gt}}$ and the registration transform $\mathbf{T}$. The second approach consists in comparing the distance between the vertebral surface points obtained from each imaging modality, known as the surface registration error (SRE). It is recommended to use a manually segmented vertebral surface in order to reduce computational bias.

This has been employed in (Chen et al., 2016) using manual surface segmentation and in (Ionescu et al., 1999; Herring et al., 1998; Muratore et al., 2002; Mozes et al., 2010; Hacihaliloglu et al., 2013b; Behnami et al., 2016) using automatic surface segmentation. Both approaches may introduce surface segmentation errors or bias in the assessment of registration accuracy, and thus a low SRE does not necessarily mean a low TRE.

7.2. Robustness

The robustness expresses how often the registration method meets the clinical requirements. Roughly speaking, while the accuracy measures how close the registration is to the ground truth, the robustness measures the fraction of times this accuracy is obtained in clinical practice. The registration robustness is measured by the success rate defined as the percentage of registration trials achieving a TRE below a given threshold. There is limited literature addressing recommendations for minimum accuracy requirements in spine interventions. In addition, the requirements vary depending on the anatomy being treated. In a study reported by Rampersaud et al. (2001), segments of the mid-cervical spine, the midthoracic spine and the thoracolumbar junction were found to have the least tolerance to screw malpositioning with a maximum tolerated error estimated to be smaller than 1 mm translation and 5° rotation. The tolerance is higher in the thoracolumbar spine, where 3.8 mm/12.7° at the L5 vertebra was estimated. In general practice, Cleary et al. (2000) suggested an accuracy of 1–2 mm to be sufficient for image-guided spine navigation. Nevertheless, there is no unique value that is universally accepted. In the context of pedicle screw fixation, the required accuracy varies significantly depending on the size of the screw, the vertebra level and the anatomy of the patient. Pedicle screw malpositioning is classified using a 2-mm increment breach grading system (Kuklo et al., 2005; Guha et al., 2017): intrapedicular, 0–2 mm breach, 2–4 mm breach and $>$ 4 mm breach. In facet joint injection, the required accuracy of the insertion channel between the articular processes of the joint is 3–5 mm (Greher et al., 2004). Typically, the threshold is set to 2 mm (Yan et al., 2011, 2012b,a; Nagpal et al., 2015; Gueziri et al., 2019), 3 mm (Rasoulian et al., 2012a; Lang et al., 2012; Gill et al., 2012; Koo and Kwok, 2016b), 3.5 mm (Khallaghi et al., 2010; Chen et al., 2016) or 4 mm (Brounstein et al., 2011; Ungi et al., 2013), depending on the clinical application. For needle insertion, clinicians often report a higher error tolerance ranging from 3 mm to 4 mm (Rasoulian et al., 2012a; Lang et al., 2012; Gill et al., 2012; Koo and Kwok, 2016b; Khallaghi et al., 2010; Chen et al., 2016; Brounstein et al., 2011; Ungi et al., 2013).

7.3. Reliability

The goal of the reliability is to assess how the registration method behaves in various experimental conditions. This is used as an indicator for the variability of the registration quality, i.e., to determine the extent/limitation in which the registration is operational. Unlike accuracy and robustness, reliability is not expressed by direct measurement. Rather, it represents the experimental design used to validate the registration. During validation, it is recommended to assess the effect of internal and external parameters on the registration quality. Internal parameters are method-specific and represent the user-defined parameters that may have a significant impact on the registration quality, e.g., the choice of the optimizer (Winter et al., 2008), the number of iUS frames (Yan et al., 2012b) or volume resolution (Gueziri et al., 2019). External parameters are common to most registration methods. The experimental design needs to involve three important external parameters:

- Initial alignment. This is used to measure the capture range of the registration method. It is achieved using a landmark-based registration (Koo and Kwok, 2016b,a) or by specifying a random transform within a given range of ±10–20 mm translation and ±10–20° rotation (Winter et al., 2008; Yan et al., 2011; Rasoulian et al., 2012a; Gill et al., 2012; Gueziri et al., 2019);
- Ultrasound data. Ultrasound parameters need to be considered, e.g, multiple ultrasound frequencies, depths and acquisition angles with complete/partial visibility of vertebrae (Winter et al., 2009; Yan et al., 2012b; Gueziri et al., 2019);
- Subject. Variability of the spine anatomy may vary significantly between individuals according to age, gender, pathology, etc. To reproduce clinical conditions, inter-subject variability needs to be taken into account (Behnami et al., 2016; Tiouririne et al., 2017; Nagpal et al., 2015; Rasoulian et al., 2012a).

7.4. Usability

In a user-centered system, the term usability is defined as a system which is easy to learn, efficient to use, easy to remember, produces low error rate and is subjectively pleasing (Nielsen, 1994). In spine navigation, usability can be seen as the extent to which the surgeon can use the IGS system to efficiently navigate. While accuracy effectiveness is measured using the TRE, time effectiveness is often related to the optimization part of the registration, excluding other intra-operative processing such as iUS acquisition time, volume reconstruction time or feature extraction time. One of the advantages of using iUS-based navigation is the rapidity at which the images can be acquired during surgery, with minimal interruption of the surgical workflow. It is crucial to consider the intra-operative time efficiency of the entire process used to achieve the registration.

Registration time requirements vary from seconds to minutes depending on the surgical procedure being performed and the application needs. While endoscopic procedures would require no more than 10–20 s to be practical, the recommended time for registration in pedicle screw fixation is under 5 minutes (Cleary et al., 2000). Spine surgeons can instrument a vertebra in 15–20 minutes in a posterior approach (Mirza et al., 2008). Any registration technique that significantly extends this time will most likely not be used by the surgeons. Moreover, if the registration procedure is meant to be performed frequently during the surgery, e.g., for frequent corrections of patient misalignment when the DRO is displaced, the time requirements need to be shortened so that the cumulative registration time remains acceptable for the surgical workflow.

8. Challenges and future directions

8.1. Ultrasound spine imaging

The quality of the iUS acquisition has a significant impact on registration accuracy. A misplaced probe or out of contact with the skin can result in partial visibility of the vertebra or shadowing artifacts. Moreover, a high body mass index can affect the image quality in percutaneous acquisition for some patients (Tiouririne et al., 2017). In the clinical assessment of their registration method, Winter et al. (2009) described a protocol for iUS acquisition including the probe specifications and the iUS imaging parameters. Although this contributes to standardize the intra-operative registrations procedure using their proposed method, there is a need for a thorough investigation of ultrasound image quality effects on the state-of-the-art registration approaches.

A subsequent topic related to conditions of imaging data concerns the growing popularity of portable ultrasound systems. The latter technology is more affordable and provides larger flexibility of use but often at the expense of a lower image quality. Existing work in spine applications that investigated feasibility of low-cost ultrasound imaging has focused on spinal curvature measurement (Yan et al., 2016) and scoliosis assessment (Cheung and Zheng, 2010). With the growing popularity of iUS-based navigation systems, evaluation of the performance for low-cost IGS outcomes is needed.

8.2. Registration type

In the context of spinal fusion surgery, most of the proposed iUS-based navigation approaches focus on rigid registration. Deformable registration also has been considered (Zettinig et al., 2017). However, allowing deformations can lead to the violation of known rigidity of the vertebra anatomy. Preservation of bone rigidity constraints has been investigated for skull and cervical vertebrae in monomodal CT registration (Al-Mayah et al., 2010; Kim et al., 2013, 2016) and CT-MR registration (Steger and Wesarg, 2012).

It has been shown that registration of individual vertebrae, in comparison to a single rigid registration of all the vertebrae, can decrease the rate of pedicle breaches (Lee et al., 2004). This is suspected to be due to the lumbar lordosis caused by posture changes during pre- and intra-operative imaging. A few papers investigated group-wise CT-to-iUS registration. Although group-wise registration involves heavier computation due to the registration of multiple vertebrae, promising results have been achieved in under 3 min computation time (Nagpal et al., 2015). An alternative approach focuses on reducing intra-operative registration time so that single vertebra alignment can be quickly performed. The idea is to render the registration procedure non-cumbersome to allow for frequent patient alignment during surgery. This is

motivated by the constant loss of accuracy reported during spine surgery (Quiñones-Hinojosa et al., 2006). Gueziri et al. (2019) demonstrated that a single vertebra can be registered under 11 s intra-operatively. Considering a typical 20–30 s to complete the iUS acquisition (Winter et al., 2009), the whole registration procedure can be achieved under 1 minute. However, the feasibility and clinical evaluation of such an approach has not been shown yet.

8.3. Effectiveness in clinical setting

While many CT/MR-to-iUS registration papers exist for spine surgery, iUS-based guidance has not become the standard of care in spine surgery for many reasons, including the significant amount of time required for iUS acquisition and registration. Many of the reviewed papers have shown satisfactory results regarding accuracy and robustness in laboratory settings, precluding the assessment of clinical conditions such as time and effort required to perform patient alignment. Although efforts are needed to further improve the accuracy and robustness, studies in clinical conditions would target the assessment of reliability and usability, highlighting the difficulties encountered in surgery. The following non-exhaustive list of research questions might help to move toward the acceptance of iUS-based navigation in the OR: Effect of ultrasound image quality–is iUS acquisition made by non-expert sonographer during surgery sufficient for good image registration? and how much training is required to perform good iUS acquisitions? Effect of visualization techniques using VR and AR setups, especially in the context of pedicle screw fixation–does AR in situ visualization of planned screw trajectory help improving the surgeon's performance? And the feasibility in terms of time effectiveness–is the iUS-based procedure easy perform during surgery? how does iUS acquisition affect the surgical workflow?

8.4. Motion monitoring

Optimized GPU implementation and high performance of hardware will likely improve the registration procedure time so that it can be executed in real-time. Solutions for continuous patient motion compensation are particularly helpful for robotic spine surgery. In the case of respiratory motion compensation or correction of patient misalignment if the DRO is displaced, due to rough surgical manipulations, or if the instrumented vertebra is far from the DRO (Guha et al., 2019a), a quick correction of the spine curvature and patient position is required. Lower thoracic and lumbar segments have been identified to be subject to significant respiratory motion ($\sim$ 2 mm) during general anaesthesia (Liu et al., 2016). Real-time acquisition and the small footprint of iUS probes make it suitable for motion monitoring. Current work in the context of robotic servoing for needle guidance has focused on using continuous iUS-to-iUS registration (Zettinig et al., 2017). For open surgery, iUS real-time monitoring has not been investigated yet.

8.5. Anatomy

The accuracy requirements vary depending on the vertebral level being treated. For cervical and thoracic levels, the required accuracy for pedicle screw fixation is estimated to be 1 mm; whereas for lumbar levels it is estimated to be 2–3 mm (Rampersaud et al., 2001). For iUS-based navigation, research has been focused on the lumbosacral region, as a substantial number of procedures involving fusion and needle guidance need to be performed in this area. Cervical, thoracic and lumbar sections present significant anatomical differences. In particular, cervical vertebrae have a smaller body, a short Y-shaped spinous process, and curved transverse processes, rendering their appearance significantly different on ultrasound imaging. To the best of our knowledge, no study reported the use of iUS-based navigation in the cervical spine.

In addition to the anatomy differences, the amount of fat and muscle tissues can be significantly different from patient to patient and at variable vertebral levels. Particularly in percutaneous iUS scans, low penetration and signal loss decrease ultrasound image quality at deeper regions, which affects the registration quality. Moreover, it is unclear to which extent does pathological tissues and fractures influence accuracy and robustness of the registration, especially in the case where the posterior bone surface is used in the registration, e.g., in feature-based registration. Further investigations involving pathological subjects need to be conducted to specify limitations of iUS-based guidance in such clinical contexts.

Non-linear and deformable registrations of soft-tissue surrounding the vertebra (e.g., muscle and nerves) are critical for tumor ablation interventions, but such approaches using iUS-based guidance have not yet been explored in the literature.

8.6. Suggestions for reporting accuracy, robustness, reliability, and usability of the registration method

In order to facilitate the comparison of different spinal navigation systems, a standardized validation method should be adopted. In such a validation standard, the accuracy needs to be based on a ground truth registration transform obtained using implanted fiducials. Each vertebral level is associated with a ground truth transform to account for any spinal curvature between pre- and intra-operative imaging. We recommend the use of 3 to 4 fiducials per vertebra. The accuracy must be reported in terms of TRE (in millimeters) and angular error (in degrees). The TRE can be computed on point of interest locations, e.g., pedicle entry points or epidural space location. The angular error can be reported by measuring the angular difference between the planned trajectory and the trajectory obtained after registration.

The robustness needs to be reported using multiple thresholds of 1 mm, 2 mm and 3 mm for the success rate of the registration. This allows to assess the registration quality for a wide range of applications according to the required accuracy. The success rate can be obtained using several repetitions of randomized starting positions ranging between ± 10 mm translation and $\pm 10^{\circ}$ rotation. Moreover, the experiment setup would involve the evaluation of the registration quality on multiple vertebral levels, using different iUS acquisitions, and using different animal and/or human cadaver specimens. The vertebral levels can be grouped into cervical, thoracic, lumbar and sacral levels as the required accuracy varies depending on the anatomical section. Multiple iUS acquisitions are used to highlight various imaging conditions including partial anatomy visibility and tilted acquisition. Multiple specimens are used to reflect the anatomical variability that can be encountered in clinical data.

The efficiency of the navigation system needs to be reported in terms of intra-operative time, i.e., the reported time should include pre-processing, initial alignment and registration times. In addition, if the validation involves assessing the contribution of a visualization technique, the efficiency time should include the operator performance time to achieve the task. This can be carried out in a user-experiment study that involves several users, well-defined tasks and user appreciation forms, to evaluate some extents of the system usability.

8.7. Future work

The evaluation of iUS-based navigation systems is challenging and involves several factors that influence the quality of the registration. There is a need for a common database that includes benchmark measurements to allow for efficient comparison of current and future registration methods based on the same criteria. Ideally, such a database should involve human and/or animal CT, MR and ultrasound data aligned with a standard fiducial-based registration that serves as the ground truth transform. The data should contain intra-operative open surgery images, as well as percutaneous images for minimally invasive surgery acquired on lumbar, thoracic and cervical regions. The success rate threshold should be clearly defined. Moreover, with the significant breakthrough made in machine learning, such a database will be a valuable resource for the development of future approaches.

While deep learning approaches have gained interest for multi-modal image registration, mostly focusing on deformable registration (Litjens et al., 2017; Shen et al., 2017), the literature of ultrasound-related registration methods is still limited. Although, in the reviewed papers, machine learning has not been directly employed to solve the registration problem, successful attempts were made to address spine-related issues, such as approximating the initial registration transform (Chen et al., 2016), segmenting the vertebra surface (Salehi et al., 2017; Baka et al., 2017; Alsinan et al., 2019) and classifying iUS images for vertebral level identification (Pesteie et al., 2015; Hetherington et al., 2017a). So far, machine learning is used as an intermediate step to achieve more *conventional* image registration techniques, mostly using a feature-based registration approach.

Future work is still needed for the acceptance of iUS-based spinal navigation in clinical routine. While the accuracy has slowly improved over 20 years (ranging from 4 mm to 1.5 mm on animal/human cadaver

studies), robustness and reliability concerns have only recently started being considered in the evaluation process. Yet, additional studies on the usability of iUS-based spinal navigation in the OR are needed. Especially, time efficiency, visualization and imaging conditions that require further investigation to identify limitations of the clinical usage.

9. Conclusion

We presented a review of the state-of-the-art techniques used in ultrasound-guided registration in spinal interventions. The registration techniques were analyzed according to a newly proposed taxonomy which is based on the surgical workflow steps: preparation of data, initialization of the registration transform, refinement of the registration and navigation. With the increasing popularity of ultrasound-guided systems for spinal interventions, the identification of a standard methodology for validation is of a crucial importance. We proposed a validation methodology based on the following four criteria. The accuracy of the system is defined as the degree of exactitude with which the instrument is located with respect to the patient anatomy or images. The robustness of the system is defined as the stability with which the registration is achieved. The reliability of the system is defined as the ability of the system to reproduce the results. Finally, the usability of the system is defined as the practicality to use the system in the clinical environment. We thoroughly discussed the significance of each criterion in the context of spinal navigation. Moreover, because many applications share similar characteristics relative to image-guided surgery, we expect these evaluation criteria to be relevant in other application contexts.

Acknowledgements

This study was funded by grants from the Canadian Institutes of Health Research (246067) and from the Natural Sciences and Engineering Research Council of Canada (396395).

References

Al-Deen Ashab, H., Lessoway, V.A., Khallaghi, S., Cheng, A., Rohling, R., Abolmaesumi, P., 2013. An augmented reality system for epidural anesthesia (area): Prepuncture identification of vertebrae. IEEE Transactions on Biomedical Engineering 60, 2636–2644.

Al-Mayah, A., Moseley, J., Hunter, S., Velec, M., Chau, L., Breen, S., Brock, K., 2010. Biomechanical-based image registration for head and neck radiation treatment. Physics in Medicine and Biology 55, 6491–6500.

Alaraj, A., Charbel, F.T., Birk, D., Tobin, M., Luciano, C., Banerjee, P.P., Rizzi, S., Sorenson, J., Foley, K., Slavin, K., et al., 2013. Role of cranial and spinal virtual and augmented reality simulation using immersive touch modules in neurosurgical training. Neurosurgery 72, A115–A123.

Alsinan, A.Z., Patel, V.M., Hacihaliloglu, I., 2019. Automatic segmentation of bone surfaces from ultrasound using a filter-layer-guided cnn. International Journal of Computer Assisted Radiology and Surgery 14, 775–783.

Amstutz, C., Caversaccio, M., Kowal, J., Bächler, R., Nolte, L.P., Häusler, R., Styner, M., 2003. A-Mode Ultrasound-Based Registration in Computer-Aided Surgery of the Skull. Archives of Otolaryngology - Head and Neck Surgery 129, 1310–1316.

Ashburner, J., Friston, K.J., 1999. Nonlinear spatial normalization using basis functions. Human Brain Mapping 7, 254.

Austin, M.S., Vaccaro, A.R., Brislin, B., Nachwalter, R., Hilibrand, A.S., Albert, T.J., 2002. Image-Guided Spine Surgery A Cadaver Study Comparing Conventional Open Laminoforaminotomy and Two Image-Guided Techniques for Pedicle Screw Placement in Posterolateral Fusion and Nonfusion Models. Spine 27, 2503–2508.

Bächler, R., Bunke, H., Nolte, L.P., 2001. Restricted surface matching—numerical optimization and technical evaluation. Computer Aided Surgery 6, 143–152.

Baka, N., Leenstra, S., van Walsum, T., 2017. Ultrasound aided vertebral level localization for lumbar surgery. IEEE Transactions on Medical Imaging 36, 2138–2147.

Barratt, D.C., Chan, C.S., Edwards, P.J., Penney, G.P., Slomczykowski, M., Carter, T.J., Hawkes, D.J., 2008. Instantiation and registration of statistical shape models of the femur and pelvis using 3D ultrasound imaging. Medical Image Analysis 12, 358 – 374.

Barratt, D.C., Penney, G.P., Chan, C.S., Slomczykowski, M., Carter, T.J., Edwards, P.J., Hawkes, D.J., 2006. Self-calibrating 3D-ultrasound-based bone registration for minimally invasive orthopedic surgery. IEEE Transactions on Medical Imaging 25, 312–323.

Behnami, D., Sedghi, A., Anas, E.M.A., Rasoulian, A., Seitel, A., Lessoway, V., Ungi, T., Yen, D., Osborn, J., Mousavi, P., Rohling, R., Abolmaesumi, P., 2017. Model-based registration of preprocedure MR and intraprocedure US of the lumbar spine. International Journal of Computer Assisted Radiology and Surgery 12, 973–982.

Behnami, D., Seitel, A., Rasoulian, A., Anas, E.M.A., Lessoway, V., Osborn, J., Rohling, R., Abolmaesumi, P., 2016. Joint registration of ultrasound, CT and a shape+pose statistical model of the lumbar spine for guiding anesthesia. International journal of computer assisted radiology and surgery 11, 937–945.

Bernstein, D.N., Brodell, D., Li, Y., Rubery, P.T., Mesfin, A., 2017. Impact of the Economic Downturn on Elective Lumbar Spine Surgery in the United States : A National Trend Analysis , 2003 to 2013. Global Spine Journal 7, 213–219.

Berton, F., Cheriet, F., Miron, M.C., Laporte, C., 2016. Segmentation of the spinous process and its acoustic shadow in vertebral ultrasound images. Computers in Biology and Medicine 72, 201–211.

Besl, P.J., McKay, N.D., 1992. A method for registration of 3-d shapes. IEEE Transactions on Pattern Analysis and Machine Intelligence 14, 239–256.

Boisvert, J., Cheriet, F., Pennec, X., Labelle, H., Ayache, N., 2008. Geometric variability of the scoliotic spine using statistics on articulated shape models. IEEE Transactions on Medical Imaging 27, 557–568.

Brendel, B., Rick, S.W.A., Stockheim, M., Ermert, H., 2002. Registration of 3D CT and Ultrasound Datasets of the Spine using Bone Structures. Computer Aided Surgery 7, 146–155.

Brendel, B., Siepermann, J., Winter, S., Ermert, H., 2005. In vivo evaluation and in vitro accuracy measurements for an ultrasound-ct registration algorithm, in: International Congress Series, pp. 583–588.

Brignol, A., Gueziri, H.E., Cheriet, F., Collins, D.L., Laporte, C., 2020. Automatic extraction of vertebral landmarks from ultrasound images: A pilot study. Computers in Biology and Medicine 122, 103838.

Brounstein, A., Hacihaliloglu, I., Guy, P., Hodgson, A., Abugharbieh, R., 2011. Towards real-time 3D US to CT bone image registration using phase and curvature feature based GMM matching. International Conference on Medical Image Computing and Computer-Assisted Intervention 14, 235–242.

Brudfors, M., Seitel, A., Rasoulian, A., Lasso, A., Lessoway, V.A., Osborn, J., Maki, A., Rohling, R.N., Abolmaesumi, P., 2015. Towards real-time, tracker-less 3D ultrasound guidance for spine anaesthesia. International Journal of Computer Assisted Radiology and Surgery 10, 855–865.

Carl, A.L., Khanuja, H.S., Sachs, B.L., Gatto, C.A., Vosburgh, K., Schenck, J., Lorensen, W., Rohling, K., Disler, D., 1997. In vitro simulation: Early results of stereotaxy for pedicle screw placement. Spine 22, 1160–1164.

Carl, B., Bopp, M., Saß, B., Pojskic, M., Gjorgjevski, M., Voellger, B., Nimsky, C., 2019a. Reliable navigation registration in cranial and spine surgery based on intraoperative computed tomography. Neurosurgical Focus FOC 47, E11.

Carl, B., Bopp, M., Saß, B., Voellger, B., Nimsky, C., 2019b. Implementation of augmented reality support in spine surgery. European Spine Journal 28, 1697–1711.

Chan, A., Coutts, B., Parent, E., Lou, E., 2020. Development and Evaluation of CT-to-3D Ultrasound Image Registration Algorithm in Vertebral Phantoms for Spine Surgery. Annals of Biomedical Engineering , 1–12.

Chen, E.C.S., Mousavi, P., Gill, S., Fichtinger, G., Abolmaesumi, P., 2010. Ultrasound guided spine needle insertion, in: Medical Imaging 2010: Visualization, Image-Guided Procedures, and Modeling, International Society for Optics and Photonics. SPIE. pp. 1028 – 1035.

Chen, F., Wu, D., Liao, H., 2016. Registration of CT and ultrasound images of the Spine with neural network and orientation code mutual information. Lecture Notes in Computer Science (including subseries Lecture Notes in Artificial Intelligence and Lecture Notes in Bioinformatics) 9805 LNCS, 292–301.

Cheung, C.W.J., Zheng, Y., 2010. Development of 3-d ultrasound system for assessment of adolescent idiopathic scoliosis (ais), in: 6th World Congress of Biomechanics (WCB 2010). August 1-6, 2010 Singapore, Springer Berlin Heidelberg, Berlin, Heidelberg. pp. 584–587.

Cideciyan, A.V., 1995. Registration of ocular fundus images: an algorithm using cross-correlation of triple invariant image descriptors. IEEE Engineering in Medicine and Biology Magazine 14, 52.

Cleary, K., Anderson, J., Brazaitis, M., Devey, G., DiGioia, A., Freedman, M., Grönemeyer, D., Lathan, C., Lemke, H., Long, D., Mun, S., Taylor, R., 2000. Final report of the technical requirements for image-guided spine procedures workshop. Computer Assisted Surgery 5, 180–215.

Collins, D.L., Evans, A.C., 1997. Animal: validation and applications of non-linear registration-based segmentation. International Journal of Pattern Recognition and Artificial Intelligence 11, 1271.

Comeau, R.M., Sadikot, A.F., Fenster, A., Peters, T.M., 2000. Intraoperative ultrasound for guidance and tissue shift correction in image-guided neurosurgery. Medical Physics 27, 787–800.

Costa, F., Dorelli, G., Ortolina, A., Cardia, A., Attuati, L., Tomei, M., Milani, D., Balzarini, L., Galbusera, F., Morenghi, E., Fornari, M., 2015. Computed tomography-based image-guided system in spinal surgerystate of the art through 10 years of experience. Operative Neurosurgery 11, 59–68.

De Nigris, D., Collins, D.L., Arbel, T., 2012. Multi-modal image registration based on gradient orientations of minimal uncertainty. IEEE Transactions on Medical Imaging 31, 2343–2354.

De Silva, T., Uneri, A., Zhang, X., Ketcha, M., Han, R., Sheth, N., Martin, A., Vogt, S., Kleinszig, G., Belzberg, A., 2018. Real-time, image-based slice-to-volume registration for ultrasound-guided spinal intervention. Physics in Medicine & Biology 63, 215016.

Desroches, G., Aubin, C.E., Sucato, D.J., Rivard, C.H., 2007. Simulation of an anterior spine instrumentation in adolescent idiopathic scoliosis using a flexible multi-body model. Medical & Biological Engineering & Computing 45, 759–768.

Di Silvestre, M., Parisini, P., Lolli, F., Bakaloudis, G., 2007. Complications of thoracic pedicle screws in scoliosis treatment. Spine 32, 1655–1661.

Echeverría, R., Cortes, C., Bertelsen, A., Macia, I., Ruiz, Ó.E., Flórez, J., 2016. Robust CT to US 3D-3D Registration by Using Principal Component Analysis and Kalman Filtering, in: Computational Methods and Clinical Applications for Spine Imaging, Springer International Publishing. pp. 52–63.

Elmi-Terander, A., Skulason, H., Söderman, M., Racadio, J., Homan, R., Babic, D., van der Vaart, N., Nachabe, R., 2016.

Surgical navigation technology based on augmented reality and integrated 3D intraoperative imaging: a spine cadaveric feasibility and accuracy study. Spine 41, E1303.
Ershad, M., Ahmadian, A., Dadashi Serej, N., Saberi, H., Amini Khoiy, K., 2014. Minimization of target registration error for vertebra in image-guided spine surgery. International journal of computer assisted radiology and surgery 9, 29–38.
Fanti, Z., Torres, F., Hazan-Lasri, E., Gastelum-Strozzi, A., Ruiz-Huerta, L., Caballero-Ruiz, A., Cosio, F.A., 2018. Improved Surface-Based Registration of CT and Intraoperative 3D Ultrasound of Bones. Journal of healthcare engineering 2018, 2365178.
Foroughi, P., Boctor, E., Swartz, M.J., Taylor, R.H., Fichtinger, G., 2007. Ultrasound Bone Segmentation Using Dynamic Programming, in: IEEE Ultrasonics Symposium Proceedings, pp. 2523–2526.
Foroughi, P., Song, D., Chintalapani, G., Taylor, R.H., Fichtinger, G., 2008. Localization of pelvic anatomical coordinate system using us/atlas registration for total hip replacement, in: International Conference on Medical Image Computing and Computer-Assisted Intervention, Springer Berlin Heidelberg, Berlin, Heidelberg. pp. 871–879.
Friston, K.J., Ashburner, J., Poline, J.B., Frith, C.D., Heather, J.D., Frackowiak, R.S.J., 1995. Spatial registration and normalization of images. Human Brain Mapping 2, 165.
Fritz, J., U-Thainual, P., Ungi, T., Flammang, A.J., Fichtinger, G., Iordachita, I.I., Carrino, J.A., 2013. Augmented reality visualisation using an image overlay system for mr-guided interventions: technical performance of spine injection procedures in human cadavers at 1.5 tesla. European Radiology 23, 235–245.
Furness, G., Reilly, M., Kuchi, S., 2002. An evaluation of ultrasound imaging for identificationof lumbar intervertebral level. Anaesthesia 57, 277–280.
Gallucci, M., Limbucci, N., Paonessa, A., Splendiani, A., 2007. Degenerative disease of the spine. Neuroimaging Clinics of North America 17, 87 – 103.
Gardner-Morse, M.G., Laible, J.P., Stokes, I.A., 1990. Incorporation of spinal flexibility measurements into finite element analysis. Journal of biomechanical engineering 112, 481–483.
Gebhard, F., Weidner, A., Liener, U.C., Stöckle, U., Arand, M., 2004. Navigation at the spine. Injury 35, 35 – 45.
Gelalis, I.D., Paschos, N.K., Pakos, E.E., Politis, A.N., Arnaoutoglou, C.M., Karageorgos, A.C., Ploumis, A., Xenakis, T.A., 2012. Accuracy of pedicle screw placement: a systematic review of prospective in vivo studies comparing free hand, fluoroscopy guidance and navigation techniques. European Spine Journal 21, 247–255.
Gill, S., Abolmaesumi, P., Fichtinger, G., Boisvert, J., Pichora, D., Borshneck, D., Mousavi, P., 2012. Biomechanically constrained groupwise ultrasound to CT registration of the lumbar spine. Medical Image Analysis 16, 662–674.
Gill, S., Mousavi, P., Fichtinger, G., Chen, E., Boisvert, J., Pichora, D., Abolmaesumi, P., 2009a. Biomechanically constrained groupwise us to ct registration of the lumbar spine, in: International Conference on Medical Image Computing and Computer-Assisted Intervention, pp. 803–810.
Gill, S., Mousavi, P., Fichtinger, G., Pichora, D., Abolmaesumi, P., 2009b. Group-wise registration of ultrasound to CT images of human vertebrae, in: Medical Imaging 2009: Visualization, Image-Guided Procedures, and Modeling, International Society for Optics and Photonics. SPIE. pp. 556 – 564.
Girardi, F.P., Cammisa, F.P.J., Sandhu, H.S., Alvarez, L., 1999. The placement of lumbar pedicle screws using computerised stereotactic guidance. The Journal of bone and joint surgery. British volume 81, 825–829.
Greher, Manfred, M., Kirchmair, Lukas, M., Enna, Birgit, M., Kovacs, Peter, M., Gustorff, Burkhard, M., Kapral, Stephan, M., Moriggl, Bernhard, M., 2004. Ultrasound-guided Lumbar Facet Nerve Block: Accuracy of a New Technique Confirmed by Computed Tomography. Anesthesiology: The Journal of the American Society of Anesthesiologists 101, 1195–1200.
Gueziri, H.E., Collins, D.L., 2019. Fast registration of ct with intra-operative ultrasound images for spine surgery, in: Computational Methods and Clinical Applications for Spine Imaging, Springer International Publishing. pp. 29–40.
Gueziri, H.E., Drouin, S., Yan, C.X.B., Collins, D.L., 2019. Toward real-time rigid registration of intra-operative ultrasound with preoperative ct images for lumbar spinal fusion surgery. International Journal of Computer Assisted Radiology and Surgery 14, 1933–1943.
Guha, D., Jakubovic, R., Gupta, S., Alotaibi, N.M., Cadotte, D., da Costa, L.B., George, R., Heyn, C., Howard, P., Kapadia, A., Klostranec, J.M., Phan, N., Tan, G., Mainprize, T.G., Yee, A., Yang, V.X., 2017. Spinal intraoperative three-dimensional navigation: correlation between clinical and absolute engineering accuracy. Spine Journal 17, 489–498.
Guha, D., Jakubovic, R., Gupta, S., Fehlings, M.G., Mainprize, T.G., Yee, A., Yang, V.X.D., 2019a. Intraoperative error propagation in 3-dimensional spinal navigation from nonsegmental registration: A prospective cadaveric and clinical study. Global Spine Journal 9, 512–520.
Guha, D., Jakubovic, R., Leung, M.K., Ginsberg, H.J., Fehlings, M.G., Mainprize, T.G., Yee, A., Yang, V.X.D., 2019b. Quantification of computational geometric congruence in surface-based registration for spinal intra-operative three-dimensional navigation. PloS one 14, e0207137.
Guimond, A., Roche, A., Ayache, N., Meunier, J., 2001. Three-dimensional multimodal brain warping using the demons algorithm and adaptive intensity corrections. IEEE Transactions on Medical Imaging 20, 58.
Haberland, N., Ebmeier, K., Grunewald, J.P., Hliscs, R., Kalff, R.L., 2000. Incorporation of intraoperative computerized tomography in a newly developed spinal navigation technique. Computer Aided Surgery 5, 18–27.
Hacihaliloglu, I., 2017. Ultrasound imaging and segmentation of bone surfaces: A review. Technology 05, 74–80.
Hacihaliloglu, I., Abugharbieh, R., Hodgson, A.J., Rohling, R.N., 2009. Bone Surface Localization in Ultrasound Using Image Phase-Based Features. Ultrasound in Medicine and Biology 35, 1475–1487.
Hacihaliloglu, I., Brounstein, A., Guy, P., Hodgson, A., Abugharbieh, R., 2012. 3D ultrasound-CT registration in orthopaedic trauma using GMM registration with optimized particle simulation-based data reduction. International Conference on Medical Image Computing and Computer-Assisted Intervention 15, 82–89.
Hacihaliloglu, I., Rasoulian, A., Rohling, R.N., Abolmaesumi, P., 2013a. Statistical Shape Model to 3D Ultrasound Registration

for Spine Interventions Using Enhanced Local Phase Features, in: International Conference on Medical Image Computing and Computer-Assisted Intervention, pp. 361–368.
Hacihaliloglu, I., Rasoulian, A., Rohling, R.N., Abolmaesumi, P., 2014. Local phase tensor features for 3-d ultrasound to statistical shape+pose spine model registration. IEEE Transactions on Medical Imaging 33, 2167–2179.
Hacihaliloglu, I., Wilson, D.R., Gilbart, M., Hunt, M.A., Abolmaesumi, P., 2013b. Non-iterative partial view 3D ultrasound to CT registration in ultrasound-guided computer-assisted orthopedic surgery. International Journal of Computer Assisted Radiology and Surgery 8, 157–168.
Hajnal, J.V., Saeed, N., Oatridge, A., Williams, E.J., Young, I.R., Bydder, G.M., 1995. Detection of subtle brain changes using subvoxel registration and subtraction of serial mr images. Journal of Computer Assisted Tomography 19, 677.
Hayes, J., Borges, B., Armstrong, D., Srinivasan, I., 2014. Accuracy of manual palpation vs ultrasound for identifying the l 3–l 4 intervertebral space level in children. Pediatric Anesthesia 24, 510–515.
Hermosillo, G., Chefd'Hotel, C., Faugeras, O., 2002. Variational methods for multimodal image matching. International Journal of Computer Vision 50, 329.
Herring, J.L., Dawant, B.M., Maurer, C.R., Muratore, D.M., Galloway, R.L., Michael Fitzpatrick, J., 1998. Surface-based registration of CT images to physical space for image-guided surgery of the spine: A sensitivity study. IEEE Transactions on Medical Imaging 17, 743–752.
Hetherington, J., Lessoway, V., Gunka, V., Abolmaesumi, P., Rohling, R., 2017a. SLIDE: automatic spine level identification system using a deep convolutional neural network. International Journal of Computer Assisted Radiology and Surgery 12, 1189–1198.
Hetherington, J., Pesteie, M., Lessoway, V.A., Abolmaesumi, P., Rohling, R.N., 2017b. Identification and tracking of vertebrae in ultrasound using deep networks with unsupervised feature learning, in: Medical Imaging 2017: Image-Guided Procedures, Robotic Interventions, and Modeling, International Society for Optics and Photonics. SPIE. pp. 159 – 165.
Heussinger, N., Eyüpoglu, I.Y., Ganslandt, O., Finzel, S., Trollmann, R., Jüngert, J., 2013. Ultrasound-guided neuronavigation improves safety of ventricular catheter insertion in preterm infants. Brain and Development 35, 905 – 911.
Hicks, J.M., Singla, A., Shen, F.H., Arlet, V., 2010. Complications of pedicle screw fixation in scoliosis surgery: a systematic review. Spine 35, E465–E470.
Ionescu, G., Lavallée, S., Demongeot, J., 1999. Automated registration of ultrasound with CT images: application to computer assisted prostate radiotherapy and orthopedics, in: International Conference on Medical Image Computing and Computer-Assisted Intervention, pp. 768–778.
Iversen, D.H., Wein, W., Lindseth, F., Unsgård, G., Reinertsen, I., 2018. Automatic intraoperative correction of brain shift for accurate neuronavigation. World Neurosurgery 120, e1071 – e1078.
Jakubovic, R., Guha, D., Gupta, S., Lu, M., Jivraj, J., Standish, B.A., Leung, M.K., Mariampillai, A., Lee, K., Siegler, P., et al., 2018. High speed, high density intraoperative 3D optical topographical imaging with efficient registration to MRI and CT for craniospinal surgical navigation. Scientific reports 8, 1–12.
Ji, S., Fan, X., Paulsen, K.D., Roberts, D.W., Mirza, S.K., Lollis, S.S., 2015. Patient registration using intraoperative stereovision in image-guided open spinal surgery. IEEE Transactions on Biomedical Engineering 62, 2177–2186.
Ji, S., Wu, Z., Hartov, A., Roberts, D.W., Paulsen, K.D., 2008. Mutual-information-based image to patient re-registration using intraoperative ultrasound in image-guided neurosurgery. Medical physics 35, 4612–4624.
Jia, R., Mellon, S.J., Hansjee, S., Monk, A.P., Murray, D.W., Noble, J.A., 2016. Automatic bone segmentation in ultrasound images using local phase features and dynamic programming, in: 2016 IEEE 13th International Symposium on Biomedical Imaging (ISBI), pp. 1005–1008.
Jia, Y., Shelhamer, E., Donahue, J., Karayev, S., Long, J., Girshick, R., Guadarrama, S., Darrell, T., 2014. Caffe: Convolutional Architecture for Fast Feature Embedding, in: Proceedings of the 22Nd ACM International Conference on Multimedia, pp. 675–678.
Kaneyama, S., Sugawara, T., Sumi, M., Higashiyama, N., Takabatake, M., Mizoi, K., 2014. A novel screw guiding method with a screw guide template system for posterior C-2 fixation: clinical article. Journal of neurosurgery. Spine 21, 231–238.
Kast, E., Mohr, K., Richter, H.P., Börm, W., 2006. Complications of transpedicular screw fixation in the cervical spine. European Spine Journal 15, 327–334.
Kerby, B., Rohling, R., Nair, V., Abolmaesumi, P., 2008. Automatic identification of lumbar level with ultrasound, in: 2008 30th Annual International Conference of the IEEE Engineering in Medicine and Biology Society, pp. 2980–2983.
Khallaghi, S., Mousavi, P., Borschneck, D., Fichtinger, G., Abolmaesumi, P., 2011. Biomechanically constrained groupwise statistical shape model to ultrasound registration of the lumbar spine, in: Information Processing in Computer-Assisted Interventions, Springer Berlin Heidelberg. pp. 47–54.
Khallaghi, S., Mousavi, P., Gong, R.H., Gill, S., Boisvert, J., Fichtinger, G., Pichora, D., Borschneck, D., Abolmaesumi, P., 2010. Registration of a Statistical Shape Model of the Lumbar Spine to 3D Ultrasound Images, in: International Conference on Medical Image Computing and Computer-Assisted Intervention, Springer Berlin Heidelberg. pp. 68–75.
Kim, B.D., Hsu, W.K., De Oliveira Jr, G.S., Saha, S., Kim, J.Y., 2014. Operative duration as an independent risk factor for postoperative complications in single-level lumbar fusion: an analysis of 4588 surgical cases. Spine 39, 510–520.
Kim, J., Matuszak, M.M., Saitou, K., Balter, J.M., 2013. Distance-preserving rigidity penalty on deformable image registration of multiple skeletal components in the neck. Medical physics 40, 121907.
Kim, J., Saitou, K., Matuszak, M.M., Balter, J.M., 2016. A finite element head and neck model as a supportive tool for deformable image registration. International Journal of Computer Assisted Radiology and Surgery 11, 1311–1317.
Koo, T.K., Kwok, W.E., 2016a. A non-ionizing technique for three-dimensional measurement of the lumbar spine. Journal of biomechanics 49, 4073–4079.
Koo, T.K., Kwok, W.E., 2016b. Hierarchical CT to Ultrasound Registration of the Lumbar Spine: A Comparison with Other

Registration Methods. Annals of Biomedical Engineering 44, 2887–2900.
Kowal, J., Amstutz, C., Langlotz, F., Talib, H., Ballester, M.G., 2007. Automated bone contour detection in ultrasound b-mode images for minimally invasive registration in computer-assisted surgery–an in vitro evaluation. International Journal of Medical Robotics and Computer Assisted Surgery 3, 341–348.
Kuklo, T.R., Lenke, L.G., O'brien, M.F., Lehman Jr, R.A., Polly Jr, D.W., Schroeder, T.M., 2005. Accuracy and efficacy of thoracic pedicle screws in curves more than 90. Spine 30, 222–226.
Lang, A., Mousavi, P., Gill, S., Fichtinger, G., Abolmaesumi, P., 2012. Multi-modal registration of speckle-tracked freehand 3D ultrasound to CT in the lumbar spine. Medical Image Analysis 16, 675–686.
Laurijssen, D., Truijen, S., Saeys, W., Daems, W., Steckel, J., 2017. An ultrasonic six degrees-of-freedom pose estimation sensor. IEEE Sensors Journal 17, 151–159.
Lee, A.J., Ranasinghe, J.S., Chehade, J.M., Arheart, K., Saltzman, B.S., Penning, D.H., Birnbach, D.J., 2011. Ultrasound assessment of the vertebral level of the intercristal line in pregnancy. Anesthesia & Analgesia 113, 559–564.
Lee, T.C., Yang, L.C., Liliang, P.C., Su, T.M., Rau, C.S., Chen, H.J., 2004. Single versus separate registration for computer-assisted lumbar pedicle screw placement. Spine 29, 1585–1589.
Leroy, A., Mozer, P., Payan, Y., Troccaz, J., 2004. Rigid Registration of Freehand 3D Ultrasound and CT-Scan Kidney Images, in: International Conference on Medical Image Computing and Computer-Assisted Intervention, Springer Berlin Heidelberg, Berlin, Heidelberg. pp. 837–844.
Litjens, G., Kooi, T., Bejnordi, B.E., Setio, A.A.A., Ciompi, F., Ghafoorian, M., van der Laak, J.A., van Ginneken, B., Sánchez, C.I., 2017. A survey on deep learning in medical image analysis. Medical Image Analysis 42, 60 – 88.
Liu, Y., Zeng, C., Fan, M., Hu, L., Ma, C., Tian, W., 2016. Assessment of respiration-induced vertebral motion in prone-positioned patients during general anaesthesia. The International Journal of Medical Robotics and Computer Assisted Surgery 12, 214–218.
Liu, Y.B., Wang, Y., Chen, Z.Q., Li, J., Chen, W., Wang, C.F., Fu, Q., 2018. Volume Navigation with Fusion of Real-Time Ultrasound and CT Images to Guide Posterolateral Transforaminal Puncture in Percutaneous Endoscopic Lumbar Discectomy. Pain physician 21, E265–E278.
Liu, Y.j., Tian, W., Liu, B., Li, Q., Hu, L., Li, Z.y., Yuan, Q., Xing, Y.g., Wang, Y.q., Sun, Y.z., 2005. [Accuracy of CT-based navigation of pedicle screws implantation in the cervical spine compared with X-ray fluoroscopy technique]. Zhonghua wai ke za zhi [Chinese journal of surgery] 43, 1328–1330.
Lou, E., Zhang, C., Le, L., Hill, D., Raso, J., Moreau, M., Mahood, J., Hedden, D., 2010. Using ultrasound to guide the insertion of pedicle screws during scoliosis surgery. Studies in health technology and informatics 158, 44–48.
Luciano, C.J., Banerjee, P.P., Bellotte, B., Oh, G.M., Lemole, Michael, J., Charbel, F.T., Roitberg, B., 2011. Learning Retention of Thoracic Pedicle Screw Placement Using a High-Resolution Augmented Reality Simulator With Haptic Feedback. Operative Neurosurgery 69, ons14–ons19.
Ma, L., Fan, Z., Ning, G., Zhang, X., Liao, H., 2018. 3D Visualization and Augmented Reality for Orthopedics, in: Intelligent Orthopaedics. Springer, pp. 193–205.
Ma, L., Zhao, Z., Chen, F., Zhang, B., Fu, L., Liao, H., 2017. Augmented reality surgical navigation with ultrasound-assisted registration for pedicle screw placement: a pilot study. International journal of computer assisted radiology and surgery 12, 2205–2215.
Merloz, P., Tonetti, J., Eid, A., Faure, C., Lavallee, S., Troccaz, J., Sautot, P., Hamadeh, A., Cinquin, P., 1997. Computer assisted spine surgery. Clinical Orthopaedics and Related Research 337, 86–96.
Michopoulou, S.K., Costaridou, L., Panagiotopoulos, E., Speller, R., Panayiotakis, G., Todd-Pokropek, A., 2009. Atlas-based segmentation of degenerated lumbar intervertebral discs from mr images of the spine. IEEE Transactions on Biomedical Engineering 56, 2225–2231.
Mirza, S.K., Deyo, R.A., Heagerty, P.J., Konodi, M.A., Lee, L.A., Turner, J.A., Goodkin, R., 2008. Development of an Index to Characterize the "Invasiveness" of Spine Surgery: Validation by Comparison to Blood Loss and Operative Time. Spine 33.
Modat, M., Ridgway, G.R., Taylor, Z.A., Lehmann, M., Barnes, J., Hawkes, D.J., Fox, N.C., Ourselin, S., 2010. Fast free-form deformation using graphics processing units. Computer methods and programs in biomedicine 98, 278–284.
Moher, D., Liberati, A., Tetzlaff, J., Altman, D.G., Group, T.P., 2009. Preferred reporting items for systematic reviews and meta-analyses: The prisma statement. PLOS Medicine 6, 1–6.
Moore, J., Clarke, C., Bainbridge, D., Wedlake, C., Wiles, A., Pace, D., Peters, T., 2009. Image guidance for spinal facet injections using tracked ultrasound, in: International Conference on Medical Image Computing and Computer-Assisted Intervention, Springer Berlin Heidelberg. pp. 516–523.
Moulder, C., Sati, M., Wentkowski, M.V., Nolte, L.P., 2003. A transcutaneous bone digitizer for minimally invasive registration in orthopedics: A real-time focused ultrasound beam approach. Computer Aided Surgery 8, 120–128.
Mozes, A., Chang, T.C., Arata, L., Zhao, W., 2010. Three-dimensional A-mode ultrasound calibration and registration for robotic orthopaedic knee surgery. International Journal of Medical Robotics and Computer Assisted Surgery 6, 91–101.
Muratore, D.M., Russ, J.H., Dawant, B.M., Galloway, R.L., 2002. Three-dimensional image registration of phantom vertebrae for image-guided surgery: A preliminary study. Computer Aided Surgery 7, 342–352.
Myronenko, A., Song, X., 2010. Point set registration: Coherent point drift. IEEE Transactions on Pattern Analysis and Machine Intelligence 32, 2262–2275.
Nagpal, S., Abolmaesumi, P., Rasoulian, A., Hacihaliloglu, I., Ungi, T., Osborn, J., Lessoway, V.A., Rudan, J., Jaeger, M., Rohling, R.N., Borschneck, D.P., Mousavi, P., 2015. A multi-vertebrae ct to us registration of the lumbar spine in clinical data. International Journal of Computer Assisted Radiology and Surgery 10, 1371–1381.
Nagpal, S., Abolmaesumi, P., Rasoulian, A., Ungi, T., Hacihaliloglu, I., Osborn, J., Borschneck, D.P., Lessoway, V.A., Rohling,

R.N., Mousavi, P., 2014. Ct to us registration of the lumbar spine: A clinical feasibility study, in: Information Processing in Computer-Assisted Interventions, Springer International Publishing. pp. 108–117.
Nielsen, J., 1994. Usability engineering. Elsevier.
Nimsky, C., Ganslandt, O., Hastreiter, P., Fahlbusch, R., 2001. Intraoperative compensation for brain shift. Surgical Neurology 56, 357 – 364.
Nkwerem, S., Goto, T., Ogiwara, T., Yamamoto, Y., Hongo, K., Ohaegbulam, S., 2017. Ultrasound-assisted neuronavigation-guided removal of a live worm in cerebral sparganosis. World Neurosurgery 102, 696.e13 – 696.e16.
O'Donnell, M., Skovoroda, A.R., Shapo, B.M., Emelianov, S.Y., 1994. Internal displacement and strain imaging using ultrasonic speckle tracking. IEEE Transactions on Ultrasonics, Ferroelectrics, and Frequency Control 41, 314–325.
Oh, T.T., Ikhsan, M., Tan, K.K., Rehena, S., Han, N.L.R., Sia, A.T.H., Sng, B.L., 2019. A novel approach to neuraxial anesthesia: application of an automated ultrasound spinal landmark identification. BMC anesthesiology 19, 57.
Oliveira, F.P., Tavares, J.M.R., 2014. Medical image registration: a review. Computer Methods in Biomechanics and Biomedical Engineering 17, 73–93.
Overley, S.C., Cho, S.K., Mehta, A.I., Arnold, P.M., 2017. Navigation and Robotics in Spinal Surgery: Where Are We Now? Neurosurgery 80, S86–S99.
Panjabi, M.M., Brand, J.R., et al., 1976. Mechanical properties of the human thoracic spine as shown by three-dimensional load-displacement curves. The Journal of bone and joint surgery. American volume 58, 642–652.
Penney, G., Barratt, D., Chan, C., Slomczykowski, M., Carter, T., Edwards, P., Hawkes, D., 2006. Cadaver validation of intensity-based ultrasound to ct registration. Medical Image Analysis 10, 385–395.
Pesteie, M., Abolmaesumi, P., Ashab, H.A.D., Lessoway, V.A., Massey, S., Gunka, V., Rohling, R.N., 2015. Real-time ultrasound image classification for spine anesthesia using local directional hadamard features. International Journal of Computer Assisted Radiology and Surgery 10, 901–912.
Pesteie, M., Lessoway, V., Abolmaesumi, P., Rohling, R.N., 2018. Automatic localization of the needle target for ultrasound-guided epidural injections. IEEE Transactions on Medical Imaging 37, 81–92.
Peters, T., Cleary, K., 2008. Image-guided interventions: technology and applications. Springer Science & Business Media.
Quiñones-Hinojosa, A., Kolen, E.R., Jun, P., Rosenberg, W.S., Weinstein, P.R., 2006. Accuracy over space and time of computer-assisted fluoroscopic navigation in the lumbar spine in vivo. Clinical Spine Surgery 19, 109–113.
Rafii-Tari, H., Abolmaesumi, P., Rohling, R., 2011. Panorama Ultrasound for Guiding Epidural Anesthesia: A Feasibility Study, in: Information Processing in Computer-Assisted Interventions, Springer Berlin Heidelberg, Berlin, Heidelberg. pp. 179–189.
Rafii-Tari, H., Lessoway, V.A., Kamani, A.A., Abolmaesumi, P., Rohling, R., 2015. Panorama Ultrasound for Navigation and Guidance of Epidural Anesthesia. Ultrasound in Medicine & Biology 41, 2220 – 2231.
Rahmathulla, G., Nottmeier, E.W., Pirris, S.M., Deen, H.G., Pichelmann, M.A., 2014. Intraoperative image-guided spinal navigation: technical pitfalls and their avoidance. Neurosurgical Focus 36, E3.
Rajaee, S.S., Delamarter, R.B., 2012. Spinal Fusion in the United States. Spine 37, 67–76.
Rampersaud, Y.R., Foley, K.T., Shen, A.C., Williams, S., Solomito, M., 2000. Radiation Exposure to the Spine Surgeon During Fluoroscopically Assisted Pedicle Screw Insertion. Spine 25, 2637–2645.
Rampersaud, Y.R., Simon, D.A., Foley, K.T., 2001. Accuracy requirements for image-guided spinal pedicle screw placement. Spine 26, 352–359.
Rasoulian, A., Abolmaesumi, P., Mousavi, P., 2012a. Feature-based multibody rigid registration of CT and ultrasound images of lumbar spine. Medical Physics 39, 3154–3166.
Rasoulian, A., Mousavi, P., Moghari, M.H., Foroughi, P., Abolmaesumi, P., 2010. Group-wise feature-based registration of CT and ultrasound images of spine, in: Medical Imaging 2010: Visualization, Image-Guided Procedures, and Modeling, International Society for Optics and Photonics. SPIE. pp. 244 – 252.
Rasoulian, A., Osborn, J., Sojoudi, S., Nouranian, S., Lessoway, V.A., Rohling, R.N., Abolmaesumi, P., 2014. A system for ultrasound-guided spinal injections: A feasibility study, in: Information Processing in Computer-Assisted Interventions, pp. 90–99.
Rasoulian, A., Rohling, R., Abolmaesumi, P., 2013a. Lumbar spine segmentation using a statistical multi-vertebrae anatomical shape+pose model. IEEE Transactions on Medical Imaging 32, 1890–1900.
Rasoulian, A., Rohling, R.N., Abolmaesumi, P., 2012b. Probabilistic registration of an unbiased statistical shape model to ultrasound images of the spine, in: Medical Imaging 2012: Image-Guided Procedures, Robotic Interventions, and Modeling, International Society for Optics and Photonics. SPIE. pp. 539 – 544.
Rasoulian, A., Rohling, R.N., Abolmaesumi, P., 2013b. Augmentation of paramedian 3D ultrasound images of the spine, in: Lecture Notes in Computer Science (including subseries Lecture Notes in Artificial Intelligence and Lecture Notes in Bioinformatics), pp. 51–60.
Rasoulian, A., Seitel, A., Osborn, J., Sojoudi, S., Nouranian, S., Lessoway, V.A., Rohling, R.N., Abolmaesumi, P., 2015. Ultrasound-guided spinal injections: a feasibility study of a guidance system. International Journal of Computer Assisted Radiology and Surgery 10, 1417–1425.
Riva, M., Hennersperger, C., Milletari, F., Katouzian, A., Pessina, F., Gutierrez-Becker, B., Castellano, A., Navab, N., Bello, L., 2017. 3D intra-operative ultrasound and MR image guidance: pursuing an ultrasound-based management of brainshift to enhance neuronavigation. International Journal of Computer Assisted Radiology and Surgery 12, 1711–1725.
Rivaz, H., Karimaghaloo, Z., Fonov, V.S., Collins, D.L., 2014. Nonrigid registration of ultrasound and mri using contextual conditioned mutual information. IEEE Transactions on Medical Imaging 33, 708–725.
Sagi, H., Manos, R., Benz, R., Ordway, N., Connolly, P., 2003. Electromagnetic field-based image-guided spine surgery part one: results of a cadaveric study evaluating lumbar pedicle screw placement. Spine 28, 2013–2018.

Salehi, M., Prevost, R., Moctezuma, J.L., Navab, N., Wein, W., 2017. Precise ultrasound bone registration with learning-based segmentation and speed of sound calibration, in: International Conference on Medical Image Computing and Computer-Assisted Intervention, pp. 682–690.

Şarlak, A.Y., Tosun, B., Atmaca, H., Sarisoy, H.T., Buluç, L., 2009. Evaluation of thoracic pedicle screw placement in adolescent idiopathic scoliosis. European Spine Journal 18, 1892.

Saß, B., Bopp, M., Nimsky, C., Carl, B., 2019. Navigated 3-Dimensional Intraoperative Ultrasound for Spine Surgery. World Neurosurgery 131, e155–e169.

Seitel, A., Sojoudi, S., Osborn, J., Rasoulian, A., Nouranian, S., Lessoway, V.A., Rohling, R.N., Abolmaesumi, P., 2016. Ultrasound-guided spine anesthesia: Feasibility study of a guidance system. Ultrasound in Medicine & Biology 42, 3043 – 3049.

Shekhar, R., Zagrodsky, V., 2002. Mutual information-based rigid and nonrigid registration of ultrasound volumes. IEEE Transactions on Medical Imaging 21, 9–22.

Shen, D., Wu, G., Suk, H.I., 2017. Deep learning in medical image analysis. Annual Review of Biomedical Engineering 19, 221–248.

Smith, Z.A., Sugimoto, K., Lawton, C.D., Fessler, R.G., 2014. Incidence of Lumbar Spine Pedicle Breach After Percutaneous Screw Fixation A Radiographic Evaluation of 601 Screws in 151 Patients. Journal of Spinal Disorders and Techniques 27, 358–363.

Solberg, O.V., Lindseth, F., Torp, H., Blake, R.E., Hernes, T.A.N., 2007. Freehand 3D Ultrasound Reconstruction Algorithms—A Review. Ultrasound in Medicine & Biology 33, 991 – 1009.

Steger, S., Wesarg, S., 2012. Automated skeleton based multi-modal deformable registration of head&neck datasets, in: International Conference on Medical Image Computing and Computer-Assisted Intervention, Springer Berlin Heidelberg. pp. 66–73.

Stiffler, K.A., Jwayyed, S., Wilber, S.T., Robinson, A., 2007. The use of ultrasound to identify pertinent landmarks for lumbar puncture. The American Journal of Emergency Medicine 25, 331–334.

Sugano, N., 2003. Computer-assisted orthopedic surgery. Journal of Orthopaedic Science 8, 442–448.

Tabaraee, E., Gibson, A.G., Karahalios, D.G., Potts, E.A., Mobasser, J.P., Burch, S., 2013. Intraoperative cone beam-computed tomography with navigation (O-ARM) versus conventional fluoroscopy (C-ARM): A cadaveric study comparing accuracy, efficiency, and safety for spinal instrumentation. Spine 38, 1953–1958.

Takahashi, S., MoriKawa, S., Saruhashi, Y., MatsUsue, Y., Kawakami, M., 2008. Percutaneous transthoracic fenestration of an intramedullary neurenteric cyst in the thoracic spine with intraoperative magnetic resonance image navigation and thoracoscopy. Journal of Neurosurgery: Spine 9, 488–492.

Takahashi, S., Saruhashi, Y., Odate, S., Matsusue, Y., Morikawa, S., 2009. Percutaneous aspiration of spinal terminal ventricle cysts using real-time magnetic resonance imaging and navigation. Spine 34, 629–634.

Talib, H., Peterhans, M., Garcia, J., Styner, M., Gonzalez Ballester, M.A., 2011. Information filtering for ultrasound-based real-time registration. IEEE transactions on bio-medical engineering 58, 531–540.

Talib, H., Rajamani, K., Kowal, J., Nolte, L.P., Styner, M., Ballester, M.A.G., 2005. A comparison study assessing the feasibility of ultrasound-initialized deformable bone models. Computer Aided Surgery 10, 293–299.

Tang, T.S.Y., Ellis, R.E., 2005. 2D/3D Deformable Registration Using a Hybrid Atlas, in: International Conference on Medical Image Computing and Computer-Assisted Intervention, Springer Berlin Heidelberg, Berlin, Heidelberg. pp. 223–230.

Tatsui, C.E., Nascimento, C.N.G., Suki, D., Amini, B., Li, J., Ghia, A.J., Thomas, J.G., Stafford, R.J., Rhines, L.D., Cata, J.P., Kumar, A.J., Rao, G., 2017. Image guidance based on mri for spinal interstitial laser thermotherapy: technical aspects and accuracy. Journal of Neurosurgery: Spine 26, 605–612.

Tiouririne, M., Dixon, A.J., Mauldin, F.W., Scalzo, D., Krishnaraj, A., 2017. Imaging Performance of a Handheld Ultrasound System with Real-Time Computer-Aided Detection of Lumbar Spine Anatomy: A Feasibility Study. Investigative Radiology 52, 447–455.

Tonetti, J., Carrat, L., Lavallee, S., Pittet, L., Merloz, P., Chirossel, J.P., 1998. Percutaneous iliosacral screw placement using image guided techniques. Clinical orthopaedics and related research , 103–110.

Ungi, T., Abolmaesumi, P., Jalal, R., Welch, M., Ayukawa, I., Nagpal, S., Lasso, A., Jaeger, M., Borschneck, D.P., Fichtinger, G., Mousavi, P., 2012. Spinal needle navigation by tracked ultrasound snapshots. IEEE Transactions on Biomedical Engineering 59, 2766–2772.

Ungi, T., Moult, E., Schwab, J.H., Fichtinger, G., 2013. Tracked ultrasound snapshots in percutaneous pedicle screw placement navigation: a feasibility study. Clinical orthopaedics and related research 471, 4047–4055.

Unsgaard, G., Rygh, O.M., Selbekk, T., Müller, T.B., Kolstad, F., Lindseth, F., Hernes, T.A.N., 2006. Intra-operative 3D ultrasound in neurosurgery. Acta Neurochirurgica 148, 235–253.

Viola, P., Jones, M.J., 2004. Robust real-time face detection. International Journal of Computer Vision 57, 137–154.

Walimbe, V., Zagrodsky, V., Raja, S., Jaber, W.A., DiFilippo, F.P., Garcia, M.J., Brunken, R.C., Thomas, J.D., Shekhar, R., 2003. Mutual information-based multimodality registration of cardiac ultrasound and spect images: a preliminary investigation. The International Journal of Cardiovascular Imaging 19, 483–494.

Wang, M., Song, Z., 2013. Optimal number and distribution of points selected on the vertebra for surface matching in CT-based spinal navigation. Computer aided surgery : official journal of the International Society for Computer Aided Surgery 18, 93–100.

Waschke, A., Walter, J., Duenisch, P., Reichart, R., Kalff, R., Ewald, C., 2013. Ct-navigation versus fluoroscopy-guided placement of pedicle screws at the thoracolumbar spine: single center experience of 4,500 screws. European Spine Journal 22, 654–660.

Wein, W., Brunke, S., Khamene, A., Callstrom, M.R., Navab, N., 2008. Automatic CT-ultrasound registration for diagnostic

imaging and image-guided intervention. Medical Image Analysis 12, 577–585.
Wein, W., Röper, B., Navab, N., 2005. Automatic registration and fusion of ultrasound with ct for radiotherapy, in: International Conference on Medical Image Computing and Computer-Assisted Intervention, Springer Berlin Heidelberg, Berlin, Heidelberg. pp. 303–311.
Whitty, R., Moore, M., Macarthur, A., 2008. Identification of the lumbar interspinous spaces: palpation versus ultrasound. Anesthesia & Analgesia 106, 538–540.
Winter, S., Brendel, B., Pechlivanis, I., Schmieder, K., Igel, C., 2008. Registration of ct and intraoperative 3-d ultrasound images of the spine using evolutionary and gradient-based methods. IEEE Transactions on Evolutionary Computation 12, 284–296.
Winter, S., Brendel, B., Rick, A., Stockheim, M., Schmieder, K., Ermert, H., 2002. Registration of bone surfaces, extracted from CT-datasets, with 3D ultrasound. Biomedizinische Technik. Biomedical engineering 47 Suppl 1, 57–60.
Winter, S., Pechlivanis, I., Dekomien, C., Igel, C., Schmieder, K., 2009. Toward registration of 3D ultrasound and CT images of the spine in clinical praxis: design and evaluation of a data acquisition protocol. Ultrasound in medicine & biology 35, 1773–1782.
Woodard, E.J., Leon, S.P., Moriarty, T.M., Quinones, A., Zamani, A.A., Jolesz, F.A., 2001. Initial experience with intraoperative magnetic resonance imaging in spine surgery. Spine 26, 410–417.
Woods, R.P., Grafton, S.T., Holmes, C.J., Cherry, S.R., Mazziotta, J.C., 1998. Automated image registration: I. general methods and intrasubject, intramodality validation. Journal of Computer Assisted Tomography 22, 139.
Wu, J.R., Wang, M.L., Liu, K.C., Hu, M.H., Lee, P.Y., 2014. Real-time advanced spinal surgery via visible patient model and augmented reality system. Computer Methods and Programs in Biomedicine 113, 869 – 881.
Xie, P., Feng, F., Cao, J., Chen, Z., He, B., Kang, Z., He, L., Wu, W., Tan, L., Li, K., et al., 2020. Real-time ultrasonography–magnetic resonance image fusion navigation for percutaneous transforaminal endoscopic discectomy. Journal of Neurosurgery: Spine 1, 1–7.
Yan, C., Tabanfar, R., Kempston, M., Borschneck, D., Ungi, T., Fichtinger, G., 2016. Comparison of portable and conventional ultrasound imaging in spinal curvature measurement, in: Medical Imaging 2016: Image-Guided Procedures, Robotic Interventions, and Modeling, International Society for Optics and Photonics. SPIE. pp. 259 – 265.
Yan, C.X., Goulet, B., Pelletier, J., Chen, S.J.S., Tampieri, D., Collins, D.L., 2011. Towards accurate, robust and practical ultrasound-CT registration of vertebrae for image-guided spine surgery. International Journal of Computer Assisted Radiology and Surgery 6, 523–537.
Yan, C.X., Goulet, B., Tampieri, D., Collins, D.L., 2012a. Ultrasound-CT registration of vertebrae without reconstruction. International Journal of Computer Assisted Radiology and Surgery 7, 901–909.
Yan, C.X.B., Goulet, B., Chen, S.J.S., Tampieri, D., Collins, D.L., 2012b. Validation of automated ultrasound-CT registration of vertebrae. International Journal of Computer Assisted Radiology and Surgery 7, 601–610.
Zettinig, O., Frisch, B., Virga, S., Esposito, M., Rienmuller, A., Meyer, B., Hennersperger, C., Ryang, Y.M., Navab, N., 2017. 3D ultrasound registration-based visual servoing for neurosurgical navigation. International journal of computer assisted radiology and surgery 12, 1607–1619.
Zhuang, B., Rohling, R., Abolmaesumi, P., 2019. Region-of-interest-based closed-loop beamforming for spinal ultrasound imaging. IEEE Transactions on Ultrasonics, Ferroelectrics, and Frequency Control 66, 1266–1280.